1
The Earth's Energy Budget and Climate Change

1.1
Introduction

The scattering and absorption of sunlight and the absorption and emission of infrared radiation by the atmosphere, land, and ocean determine the Earth's climate. In studies of the Earth's atmosphere, the term *solar radiation* is often used to identify the light from the sun that illuminates the Earth. Most of this radiation occupies wavelengths between 0.2 and 5 μm. Throughout this book the terms "sunlight, solar radiation, and shortwave radiation" are used interchangeably. Light perceivable by the human eye, visible light, occupies wavelengths between 0.4 and 0.7 μm, a small portion of the incident sunlight. Similar to the terminology used for solar radiation, throughout this book the terms "emitted radiation, terrestrial radiation, thermal radiation, infrared radiation, and longwave radiation" are used interchangeably for thermal radiation associated with terrestrial emission by the Earth's surface and atmosphere. Most of the emission occupies wavelengths between 4 and 100 μm.

Sunlight heats the Earth. Annually averaged, the rate at which the Earth absorbs sunlight approximately balances the rate at which the Earth emits infrared radiation to space. This balance sets the Earth's global average temperature. Most of the incident sunlight falling on the Earth is transmitted by the atmosphere to the surface where a major fraction of the transmitted light is absorbed. Annually averaged, the surface maintains its global average temperature by balancing the rates at which it absorbs radiation and loses energy to the atmosphere. Most of the loss is due to the emission of infrared radiation by the surface. Unlike its relative transparency to sunlight, the atmosphere absorbs most of the infrared radiation emitted by the surface. The atmosphere in turn maintains its average vertical temperature profile through the balance of radiation absorbed; the release of latent heat as water vapor condenses, freezes, and falls as precipitation; the turbulent transfer of energy from the surface; and the radiation emitted by clouds and by the greenhouse gases, gases that absorb infrared radiation.

This chapter begins with the global annually averaged balance between the sunlight absorbed by the Earth and the infrared radiation emitted to space. A simple radiative equilibrium model for the Earth renders a global average

Atmospheric Radiation: A Primer with Illustrative Solution, First Edition.
James A. Coakley Jr and Ping Yang.

temperature that is well below freezing, even if the Earth absorbed substantially more sunlight than it currently absorbs. The Earth's atmosphere is modeled as one that allows sunlight to pass through but blocks the infrared radiation that is emitted by the surface. This simple model produces the Earth's greenhouse effect leading to a warm, habitable surface temperature. The model provides an estimate of the radiative response time for the Earth's atmosphere, about a month. The month-long response time explains the atmosphere's relative lack of response to the day–night variation in sunlight and also its sizable response to seasonal shifts as the Earth orbits the sun. The model also leads to estimates of changes in the average temperature caused by changes in the incident sunlight and in atmospheric composition, such as the buildup of carbon dioxide in the atmosphere from the burning of fossil fuels. Some of the change in temperature is due to feedbacks in the atmosphere and surface that alter the amounts of sunlight absorbed and radiation emitted as the Earth's temperature changes. This chapter then describes more realistic models for the Earth's atmosphere considered as a column of air with a composition close to the global average composition. It describes how forcing the atmosphere to be in radiative equilibrium leads to turbulent heat exchange between the atmosphere and the surface. The combination of radiation and the exchange with the surface largely explains the vertical structure of the Earth's global average temperature. In addition, the chapter describes realistic estimates for the various sources of heating and cooling for the surface and the atmosphere and the roles played by clouds and the major radiatively active gases. The chapter ends by noting that the distribution of the incident sunlight with latitude leads to the complex circulations of the atmosphere and oceans. The winds associated with the atmospheric circulation and the accompanying pattern of precipitation and evaporation contribute to the circulation of the oceans. The winds and ocean currents carry energy from the tropics to high latitudes. This transfer of energy moderates the temperatures of both regions.

1.2 Radiative Heating of the Atmosphere

The first law of thermodynamics states that energy is conserved. According to this law, an incremental change in the internal energy of a small volume of the atmosphere dU is equal to the heat added dQ minus the work done by the air dW.

$$dU = dQ - dW \tag{1.1}$$

Air behaves similarly to an ideal gas. For an ideal gas the internal energy is proportional to the absolute temperature. An incremental change in internal energy is given by $dU = mC_V\,dT$ with m the mass of air undergoing change and C_V the heat capacity of air held at a constant volume. Of course, the atmosphere is free to expand and contract. It is not confined to a volume. Held at constant pressure, air will expand if its temperature rises. The work done by the air is $P\,dV$ with P the pressure of the air and dV the incremental change in its volume. Combining the

equation of state for an ideal gas $PV = mRT$ with the conservation of energy gives

$$mC_p\,dT = dQ + \frac{mRT}{P}dP \tag{1.2}$$

with $C_p = 1005\,\mathrm{J\,kg^{-1}\,K^{-1}}$ being the heat capacity of air held at constant pressure, $C_P = C_V + R$, and $R = 287\,\mathrm{J\,kg^{-1}\,K^{-1}}$ the gas constant for dry air. Throughout this book, the small changes sometimes applied to the temperature in order to account for the effects of water vapor on the heat capacity and gas constant will be ignored. For a small increment in time, *dt,*

$$mC_p\frac{dT}{dt} = \frac{dQ}{dt} + \frac{mRT}{P}\frac{dP}{dt} \tag{1.3}$$

with dT/dt often referred to as the *heating rate* and often expressed in units of Kelvin per day, dQ/dt being the rate at which energy is being added or removed from the air ($\mathrm{J\,s^{-1}}$ or W), and dP/dt the rate at which the pressure of the air is changing. The pressure changes give rise to motion. Air responds to heating by changing its temperature and moving. Most of the radiative heating in the atmosphere goes to changing the thermodynamic state, such as the temperature changes experienced in high latitudes in response to changes in solar heating as the Earth orbits the sun. There are, however, some instances in which the radiative heating nearly balances the dynamical response. The rate of downward motion referred to as *subsidence* approximately matches the radiative cooling in the troposphere of subtropical high pressure systems. For annual mean, global average conditions, there is no net movement of air, $dP/dt = 0$. Consequently,

$$mC_p\frac{dT}{dt} = \frac{dQ}{dt} \tag{1.4}$$

1.3 Global Energy Budget

Annually averaged, the Earth approximately maintains a state of radiative equilibrium. Under such conditions, the annually averaged, global mean temperature remains constant with time. For radiative equilibrium, the rate at which the Earth absorbs sunlight equals the rate at which the Earth emits radiation.

Let Q_0 be the solar constant in units of power per unit area ($\mathrm{W\,m^{-2}}$), the sunlight reaching the "top" of the Earth's atmosphere at the average distance between the Earth and the sun, one astronomical unit (AU). There is, of course, no "top" of the atmosphere. Instead, the top represents the surface of an imaginary sphere that contains the Earth and most of the atmosphere. Here, the sphere contains the atmosphere that absorbs or reflects a major fraction of the incident sunlight and also absorbs and emits a major fraction of the infrared radiation. A sphere with a radius that extends to 30 km above the Earth's surface serves as an imaginary "top." Such a sphere contains 99% of the Earth's atmosphere.

The solar constant has been measured with high accuracy (~0.1%) from satellites. The measured values range roughly from 1360 to $1370\,\mathrm{W\,m^{-2}}$. The

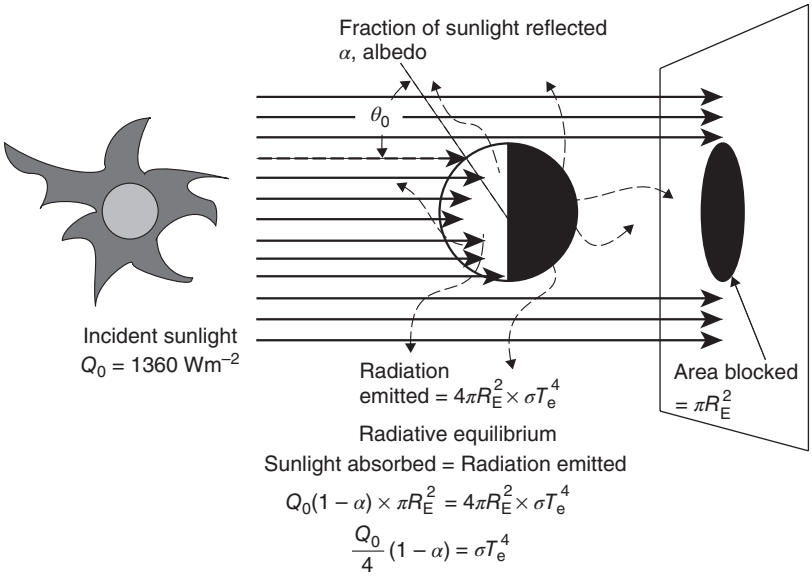

Figure 1.1 Radiative equilibrium for the Earth. The rays from the sun are parallel as they strike the Earth. To a distant viewer in space, the Earth casts a shadow as if it were a circle having a radius equal to that of the Earth. The Earth reflects a fraction of the sunlight that is blocked and absorbs the remainder. In radiative equilibrium, the absorbed sunlight is balanced by the emitted infrared radiation. The Earth rotates sufficiently rapidly that its radiative equilibrium temperature, T_e, is assumed to be the same for both day and night sides. The angle between the incident sunlight and the normal of the Earth's surface where the sunlight strikes is the solar zenith angle θ_0.

most recent measurements [1] are thought to provide the most accurate value, 1361 W m^{-2}. Moreover, the solar constant is not constant, but varies with the 11 year cycle of sunspots. The peak-to-peak amplitude of the solar constant variation is about 0.2% of the average value. For convenience, $Q_0 = 1360\,\mathrm{W\,m^{-2}}$ is used unless otherwise noted. In addition, the distance between the Earth and the sun is far greater than both the radius of the Earth and the radius of the sun. As a result, the solar radiation incident on the Earth appears as if it were collimated so that the rays of incident sunlight are all parallel to a line joining the centers of the sun and the Earth, as shown in Figure 1.1.

If the Earth were to absorb all sunlight incident on its surface, the rate of absorption would be $Q_0 \pi R_E^2$ with $R_E = 6371$ km the Earth's radius. As shown in Figure 1.1, the area of the circle πR_E^2 is the area blocked by the Earth as it passes between the sun and a distant observer in space. The Earth does not absorb all of the incident sunlight. It reflects a fraction. The albedo α is the fraction of sunlight reflected. It too has been measured from satellites and has been found to be close to 0.3 [2]. The fraction of sunlight absorbed is thus $1 - \alpha$. Finally, the Earth is approximately a sphere. Only half is being illuminated at any instant. For that half, the average sunlight incident per unit area is given by $Q_0/2 = 680\,\mathrm{W\,m^{-2}}$. The fractional factor

"1/2" represents the ratio of the area of the circle that blocks the sunlight to the surface area of the hemisphere having the same radius. The fractional factor also represents the global average cosine of the solar zenith angle for the sunlit side of the Earth. Zenith is the upward direction normal to the Earth's surface. The solar zenith angle at the surface of the Earth is the angle between the upward normal of the Earth's surface and the direction to the sun as illustrated in Figure 1.1. The cosine of the solar zenith angle accounts for the slant of the Earth's surface away from the direction of the incident rays of sunlight. Owing to the slant angle, the solar radiation at the top of the atmosphere is distributed over the larger area of the slanted surface. The power per unit area is diminished by the cosine of the solar zenith angle. For the sunlit side of the Earth an "effective" average solar zenith angle is that which produces the average cosine of the solar zenith angle, 60°. As discussed later in this chapter, the Earth spins rapidly on its axis so that on average, the absorbed sunlight is distributed over both the dayside and the nightside. The global average incident sunlight becomes $Q_0/4 = 340\,\mathrm{W\,m^{-2}}$. The division by 4 is obtained by invoking the ratio of the area of a circle with a given radius to that of a sphere with the same radius. The same result is obtained by calculating the average cosine of the solar zenith angle for the daylight side of a sphere illuminated by sunlight and dividing the average cosine by two to obtain the "day–night average" incident solar radiation for a rapidly rotating sphere.

The rate of emission by the Earth is assumed to be that of a blackbody and is given by the Stefan–Boltzmann law. Assuming that the Earth's temperature is everywhere the same, the rate of emission is given by σT_e^4 with $\sigma = 5.67 \times 10^{-8}\,\mathrm{Wm^{-2}\,K^{-4}}$ the Stefan–Boltzmann constant and T_e the radiative equilibrium temperature or the effective radiating temperature of the Earth. In Figure 1.1 the emission is symbolically portrayed by the curved dashed lines emanating from the Earth. In radiative equilibrium, the rate at which radiation is absorbed equals the rate at which radiation is emitted.

$$\frac{Q_0}{4}(1-\alpha) = \sigma T_e^4 \tag{1.5}$$

The radiative equilibrium temperature for the Earth is given by

$$T_e = \left[\frac{Q_0\,(1-\alpha)}{4\sigma}\right]^{1/4} = \left[\frac{1360\,\mathrm{Wm^{-2}} \times (1-0.3)}{4 \times 5.67 \times 10^{-8}\,\mathrm{Wm^{-2}\,K^{-4}}}\right]^{1/4} = 255\,\mathrm{K} \tag{1.6}$$

The equilibrium temperature is equivalent to an atmospheric temperature at an altitude of about 5 km. Suppose there were no atmosphere and the Earth was entirely covered by oceans. The albedo of the earth would be that of the oceans, $\alpha = 0.06$. Then the radiative equilibrium temperature would be

$$T_e = \left[\frac{1360\,\mathrm{Wm^{-2}} \times (1-0.06)}{4 \times 5.67 \times 10^{-8}\,\mathrm{Wm^{-2}\,K^{-4}}}\right]^{1/4} = 274\,\mathrm{K} \tag{1.7}$$

The Earth would be close to freezing.

1.4 The Window-Gray Approximation and the Greenhouse Effect

The window-gray, radiative equilibrium model of the Earth is the simplest model that contains the greenhouse effect. The greenhouse effect of the Earth's atmosphere represents the difference between the radiative equilibrium temperature and the Earth's surface temperature. In this book, 288 K is used for the global, annually averaged surface temperature, approximately its current value. The warm surface arises from the Earth's atmosphere transmitting most of the incident sunlight to the surface. The surface absorbs most of this transmitted sunlight. Only a small fraction of the incident sunlight is absorbed by the atmosphere. Unlike its transparency to sunlight, the Earth's atmosphere absorbs a large fraction of the infrared radiation emitted by the surface. In the window-gray, radiative equilibrium model, the atmosphere is transparent for incident sunlight, but equally absorbing at all wavelengths for infrared radiation. The term "gray" means no color, or equivalently, no variation of the radiation with wavelength. Clouds reflect light and transmit light equally at all wavelengths in the visible spectrum and thus appear to be of various shades of gray from black or dark gray to white.

In the window-gray approximation, sunlight passes through the atmosphere and the fraction that is not reflected is absorbed by the surface. Thus, the surface albedo is assumed to be the same as the Earth's albedo, $\alpha = 0.3$. In addition, the atmosphere is taken to be isothermal, meaning that it has the same temperature at all altitudes. Furthermore, the atmosphere is also assumed to be in radiative equilibrium. For an isothermal atmosphere in radiative equilibrium, the fraction of radiation absorbed, which is given by an absorptivity, is equal to the fraction of radiation emitted, which is given by an emissivity. This conclusion can be derived from the second law of thermodynamics and is known as *Kirchoff's radiation law* after Gustav R. Kirchoff who first noted this relationship in the latter half of the nineteenth century [3]. Only three things can happen to light as it passes through an atmosphere. It can be reflected by objects that scatter light. It can be absorbed, and it can be transmitted. Assuming that none of the infrared radiation is scattered so that there is no reflection, in order to conserve energy at infrared wavelengths, radiation not absorbed is transmitted. Since the fraction of radiation absorbed is given by the emissivity ϵ, the fraction of radiation transmitted is given by $1 - \varepsilon$. Figure 1.2 illustrates the energy exchanges for the Earth, the atmosphere, and the surface in the window-gray approximation.

The window-gray, radiative equilibrium model gives rise to two equations with two unknowns, the temperature of the surface T_S, and the temperature of the isothermal atmosphere T_A. At the top of the atmosphere, radiative equilibrium for the Earth leads to

$$\frac{Q_0}{4}(1-\alpha) = \varepsilon\sigma T_A^4 + (1-\varepsilon)\sigma T_S^4 \tag{1.8}$$

At the surface, radiative equilibrium of the surface leads to

$$\frac{Q_0}{4}(1-\alpha) + \varepsilon\sigma T_A^4 = \sigma T_S^4 \tag{1.9}$$

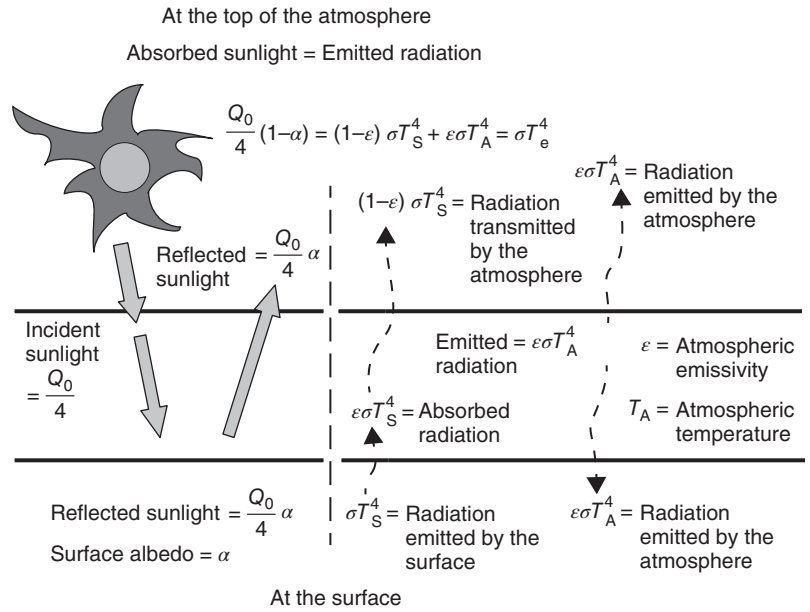

Absorbed sunlight + Radiation emitted by the atmosphere and absorbed by the surface = Radiation emitted by the surface

$$\frac{Q_0}{4}(1-\alpha) + \varepsilon\sigma T_A^4 = \sigma T_S^4$$

Figure 1.2 Window-gray, radiative equilibrium model.

Notice that in Equation 1.9, the surface absorbs all of the radiation that it does not reflect. In radiative equilibrium the surface emits at the same rate that it absorbs radiation. The fraction absorbed is equal to the fraction emitted, which in Equation 1.9 is assumed to be unity. For most surfaces on Earth, the emissivity is close to unity. For simplicity, unit surface emissivity is assumed throughout this book. Substituting Equation 1.5 into Equation 1.9 yields

$$\sigma T_S^4 = \sigma T_e^4 + \varepsilon\sigma T_A^4 \tag{1.10}$$

Consequently, $T_S > T_e$. The surface has a higher temperature owing to the presence of an atmosphere that absorbs infrared radiation. Subtracting Equation 1.8 from Equation 1.9 leads to the radiative equilibrium condition for the atmosphere

$$\varepsilon\sigma T_S^4 = 2\varepsilon\sigma T_A^4 \tag{1.11}$$

Clearly, the atmosphere is at a lower temperature than the surface. Substituting Equation 1.11 into Equation 1.9 yields the surface temperature as given by

$$T_S = \left[\frac{Q_0 (1 - \alpha)}{4\sigma \left(1 - \frac{\varepsilon}{2}\right)} \right]^{1/4} \tag{1.12}$$

For the Earth, $T_S = 288\,\text{K}$. With this surface temperature, Equation 1.11 gives the temperature of the atmosphere as $T_A = 242\,\text{K}$. Using $T_S = 288\,\text{K}$, $\alpha = 0.3$, and $Q_0 = 1360\,\text{W m}^{-2}$, and solving Equation 1.12 to obtain a consistent value for the emissivity yields $\varepsilon = 0.78$.

Like the Earth's atmosphere, the window-gray atmosphere is heated by the surface, and the primary source of atmospheric heating is the absorption of infrared radiation emitted by the surface. Clearly from Equation 1.12, if the absorption of longwave radiation in the atmosphere increases, ϵ increases and the surface temperature rises. Owing to the condition of radiative equilibrium, which leads to Equation 1.11, as the surface temperature rises, the atmospheric temperature must also rise.

With no atmosphere, the Earth's surface temperature would equal the radiative equilibrium temperature. If the Earth had an albedo of 0.3 without an atmosphere, then the surface temperature would be 255 K. Because the atmosphere absorbs infrared radiation, the Earth's surface temperature is 288 K. The difference, $288 - 255\,\text{K} = 33\,\text{K}$, is the greenhouse effect. The surface temperature is 33 K higher than it would be if the atmosphere were transparent at infrared wavelengths and the Earth had an albedo of 0.3. The difference between emission by the Earth's surface and that at the top of the atmosphere, $390 - 240\,\text{W m}^{-2} = 150\,\text{W m}^{-2}$, is referred to as the *greenhouse forcing*. The greenhouse forcing may be considered as a climate forcing similar to those due to the buildup of greenhouse gases in the atmosphere, which is discussed in the next section. Since the radiation emitted at the top of the atmosphere and by the surface are both measurable, and since the 33 K response is observed, the ratio of the greenhouse effect to the greenhouse forcing provides an empirical estimate of climate sensitivity.

$$\frac{33\,\text{K}}{150\,\text{W m}^{-2}} \sim 0.2\,\text{K}\,(\text{W m}^{-2})^{-1} \tag{1.13}$$

Climate sensitivity is the equilibrium response of the surface temperature that results from a constant radiative forcing. For a climate forcing of $1\,\text{W m}^{-2}$ and a sensitivity of $0.2\,\text{K}\,(\text{W m}^{-2})^{-1}$, the response would be 0.2 K. This sensitivity is about a factor of three smaller than the sensitivity expected for the Earth's climate.

1.5 Climate Sensitivity and Climate Feedbacks

For the Earth's temperature to remain constant, the Earth must maintain a state of radiative equilibrium; the amount of absorbed sunlight must equal the amount

of radiation emitted, indicated here by a variable F.

$$\frac{Q_0}{4}(1-\alpha) = F \tag{1.14}$$

If the composition of the atmosphere is changed, as when a volcano erupts and the stratosphere is filled with tiny droplets of sulfuric acid and tiny particles of sulfate that reflect sunlight, then the current state of radiative equilibrium is upset. The climate will respond to the change so that a new state of radiative equilibrium is established. The rate at which the Earth is heated is given by

$$mC_P\frac{dT}{dt} = \Delta\left[\frac{Q_0}{4}(1-\alpha) - F\right] = \Delta\mathscr{R}_{\mathrm{NET}} \tag{1.15}$$

The term in the brackets in Equation 1.15 is the change in the net radiation budget of the Earth, $\Delta\mathscr{R}_{\mathrm{NET}}$. It is the change in the rate at which sunlight is absorbed minus the change in the rate at which the Earth emits. The change in the net radiation budget is referred to as the *radiative forcing* of the climate.

The symbols in Equation 1.15 for the mass and heat capacity are the same as those used for the atmosphere in Equations 1.3 and 1.4. Their product gives the "thermal inertia" of the atmosphere. A more appropriate mass and heat capacity for the Earth, however, are those associated with the elements of the system that undergo substantial temperature change over periods of a few years. For periods of a few years, the largest thermal inertia is associated with the uppermost 50 – 100 m of the ocean known as the *ocean mixed layer*. This layer of water is stirred by surface winds so that its temperature is nearly uniform throughout. For decadal and longer scales, the temperature of the deep ocean also changes but such changes will be ignored in this analysis. Since the thermal inertia of the ocean mixed layer is much larger than that of the overlying atmosphere, atmospheric surface temperatures, and thus mean atmospheric temperatures, are tied to ocean surface temperatures. For land surfaces, however, soils, asphalt, concrete, and vegetation are poor heat conductors. As a result, relatively little mass is involved in temperature changes of land surfaces. Lack of heat capacity is the reason that land surface temperatures respond so dramatically to the daily cycle of solar heating. Since the thermal inertia of the atmosphere is much greater than that involved in changing land surface temperatures, land surface temperatures averaged over several years tend to follow the average temperature of the overlying atmosphere.

The term in brackets in Equation 1.15 gives the net radiative heating. It is zero when the Earth is in equilibrium. For a volcanic eruption, the equilibrium can be broken. The albedo increases, less sunlight is absorbed, and the Earth cools. Alternatively, as indicated for the window-gray, radiative equilibrium model, if the infrared absorption by the Earth's atmosphere is suddenly increased, the emission at the top of the atmosphere as given by Equations 1.8, 1.11, and 1.14, $F = (1 - \varepsilon/2)\sigma T_S^4$, decreases and the Earth warms.

The equilibrium response to a radiative forcing is approximately given by a Taylor series expansion of the brackets in Equation 1.15:

$$(1-\alpha_0)\frac{\Delta Q_0}{4} - \frac{Q_0}{4}\left(\left.\frac{\partial\alpha}{\partial U}\right|_{T_S}\Delta U + \left.\frac{\partial\alpha}{\partial T_S}\right|_{U}\Delta T_S\right) - \left.\frac{\partial F}{\partial T_S}\right|_{U}\Delta T_S - \left.\frac{\partial F}{\partial U}\right|_{T_S}\Delta U = 0 \tag{1.16}$$

with α_0 the albedo for the current equilibrium climate and ΔQ_0 a change in the incident solar radiation. As was noted earlier, the incident solar radiation is not constant. It changes slightly over the course of the 11 year sunspot cycle and is thought to have longer term variations of a few tenths of a percent on century to millennial scales. Such changes are relatively small compared with other sources of forcing. For the present, these changes are taken to be negligibly small, $\Delta Q_0 = 0$. The change in albedo due to a change in atmospheric composition, such as that brought about by a volcanic eruption, is given by $(\partial\alpha/\partial U)\Delta U$. A similar term could be used for a change in the albedo due to human practices, such as clearing of forests to create croplands. The change in the albedo due to surface temperature is given by $(d\alpha/dT_S)\Delta T_S$. The term includes climate feedbacks, such as the decrease in area covered by snow and ice as the Earth's temperature rises, as is observed [4], and changes in cloud properties with the Earth's temperature. For the emitted infrared radiation, the terms are similar. Changes in the emitted radiation due to changes in atmospheric composition are given by $(dF/dU)\Delta U$. Changes in atmospheric composition arise from human activity, such as the buildup of carbon dioxide in the atmosphere from the burning of fossil fuels. The change in the emitted radiation with temperature is given by $(dF/dT_S)\Delta T_S$. It includes not only the rise in emission with increasing temperature of the surface and atmosphere but also feedbacks such as, for example, the increase in the concentration of atmospheric water vapor as the Earth's temperature rises and changes in the emitted radiation due to changes in cloud properties as the Earth's temperature changes. The emitted radiation also varies from what appear to be natural causes. An example of natural variations is the increase and decrease in carbon dioxide and methane concentrations in the atmosphere as the Earth thaws from an ice age and then cools as it enters another ice age. Such changes are thought to arise from the thawing and freezing of permafrost and other biological changes that could accompany a warming and cooling Earth. Whether to call such changes a forcing or a feedback is usually determined by how rapidly the feedback alters the climate. Evidence from the paleoclimate record suggests that since the start of the industrial revolution, changes in atmospheric composition due to human activity far outpace any changes that occurred during the thousands of years over which the Earth recovered from the last ice age [4]. Also, changes in vegetation surely accompany climate change, such as the transition from forests to grasslands and grasslands to shrubs and deserts. Such transitions, however, are expected to be relatively slow, decades to century scales. They are much slower than the faster changes expected in the hydrologic cycle, the buildup of water vapor with increasing temperature, decreases in seasonal snow and ice cover,

and changes in cloud properties. Changes in the hydrologic cycle have short time scales, typically shorter than seasonal scales. In addition, the biological changes seem to respond to multiyear trends in temperatures and the hydrologic cycle. The feedbacks normally included in estimates of climate sensitivity are those associated with the hydrologic cycle [5].

Consider the equilibrium response of the surface temperature to the eruption of Mt. Pinatubo in June 1991. From Equation 1.16 the change in the net radiation budget becomes

$$-\frac{Q_0 \Delta\alpha_U}{4} - \Delta F_U = \left(\frac{\partial F}{\partial T_S} + \frac{Q_0}{4} \frac{\partial \alpha}{\partial T_S} \right) \Delta T_S \tag{1.17}$$

with $\Delta\alpha_U = (\partial\alpha/\partial U)\Delta U$ representing the change in albedo caused by the buildup of the volcanic haze layer in the stratosphere and $\Delta F_U = (\partial F/\partial U)\Delta U$ representing the change in emitted radiation caused by the layer. Initially, the haze layer affected the emitted infrared radiation, but with time, the large ash and clay particles that were part of the initial plume fell from the stratosphere, leaving the small droplets of sulfuric acid and particles of sulfate behind. While the remaining volcanic layer also had an effect on the emitted infrared radiation, the effect was relatively small compared with the effect of the particles on the reflected sunlight. For simplicity, the effects of the haze layer on emitted radiation will be ignored, $\Delta F_U = 0$. From Equation 1.17 the change in the equilibrium temperature is given by

$$\Delta T_S = \frac{-\dfrac{Q_0 \Delta\alpha_U}{4}}{\dfrac{Q_0}{4} \dfrac{\partial \alpha}{\partial T_S} + \dfrac{\partial F}{\partial T_S}} \tag{1.18}$$

Aside from the effects of clouds, the emitted radiation is expected to increase with increasing temperatures, $\partial F/\partial T_S > 0$. Likewise, aside from the effects of clouds and because there is less ice and snow as the temperature rises, the albedo will decrease. In addition, as discussed in Section 1.7, the atmosphere appears to maintain a state in which the relative humidity remains approximately constant. Consequently, as the temperature rises, the amount of atmospheric water vapor increases, thereby increasing the absorption of sunlight and further decreasing the albedo. So, as the temperature rises, $\partial\alpha/\partial T_S < 0$. Numerical estimates indicate that $Q_0/4\ \partial\alpha/\partial T_S + \partial F/\partial T_S > 0$. With the denominator in Equation 1.18 greater than zero, an increase in albedo causes a decrease in the surface temperature. A decrease was observed following the Mt. Pinatubo eruption [4].

Following the same strategy starting with Equation 1.16, if carbon dioxide in the atmosphere were to suddenly double, the emission at the top of the atmosphere would fall by about 4 W m^{-2}, $\Delta F_U = -4$ W m^{-2} in Equation 1.17. Since the increase in carbon dioxide has almost no effect on the absorbed sunlight, $\Delta\alpha_U = 0$. As a result, the change in the equilibrium temperature for an increase in carbon dioxide would be given by

$$\Delta T_S = \frac{-\Delta F_U}{\dfrac{Q_0}{4} \dfrac{\partial \alpha}{\partial T_S} + \dfrac{\partial F}{\partial T_S}} \tag{1.19}$$

Thus, the temperature will increase for a doubling of CO_2.

For the window-gray, radiative equilibrium model, the planetary albedo, which is the same as the surface albedo, remains constant, $\partial\alpha/\partial T_S = 0$. In addition, the emissivity of the atmosphere remains constant so that

$$\frac{\partial F}{\partial T_S} = \frac{\partial\left(1-\frac{\varepsilon}{2}\right)\sigma T_S^4}{\partial T_S} = \frac{4\left(1-\frac{\varepsilon}{2}\right)\sigma T_S^4}{T_S} = \frac{4\times 240}{288}\,\mathrm{W\,m^{-2}K^{-1}} = 3.3\,\mathrm{W\,m^{-2}K^{-1}} \tag{1.20}$$

As a result, the response of the surface temperature to a change in atmospheric composition, or for that matter, a change in the solar constant, is given by

$$\Delta T_S = \beta \Delta \mathscr{R}_{NET} \tag{1.21}$$

with $\Delta\mathscr{R}_{NET}$ the change in the radiation budget at the top of the atmosphere. The change in the top of the atmosphere radiation budget is the radiative forcing ($\mathrm{W\,m^{-2}}$). The climate sensitivity β is the inverse of the denominator in Equation 1.19. For the window-gray, radiative equilibrium model, $\beta = 0.3\,\mathrm{K\,W^{-1}\,m^{-2}}$. This value is close to the $0.2\,\mathrm{K\,W^{-1}\,m^{-2}}$ estimated from the greenhouse forcing and the greenhouse effect of the Earth's atmosphere. For a doubling of CO_2, the response would be $\Delta T_S = 1.2\,\mathrm{K}$. This same response was obtained in an early model for the Earth's atmosphere in which the amount of water vapor was held fixed so that the emissivity of the atmosphere also remained constant [6].

For the Earth's atmosphere, the relative humidity appears to remain fairly constant. Numerical simulations in which clouds, surface reflection, and relative humidity in the atmosphere are held constant give $Q_0/4\ \partial\alpha/\partial T_S = -0.2\,\mathrm{W\,m^{-2}K^{-1}}$. With the relative humidity fixed, the rise in the atmospheric temperature is accompanied by a rise in water vapor. The change in albedo results from the slight increase in the absorption of sunlight as the amount of water vapor increases. For emitted radiation, $\partial F/\partial T_S = 2\,\mathrm{W\,m^{-2}K^{-1}}$. The sensitivity of the emitted radiation is smaller than that for the window-gray model owing to the changes in water vapor. This change in water vapor with a change in temperature is referred to as the *water vapor feedback* in the climate system. With fixed relative humidity, $\beta = 0.6\,\mathrm{K\,W^{-1}\,m^{-2}}$. For a doubling of CO_2, the response is $\Delta T_S = 2.4\,\mathrm{K}$, twice the value obtained for the window-gray model [7] and three times the sensitivity estimated from the greenhouse forcing and the greenhouse effect.

1.6 Radiative Time Constant

The window-gray model lends itself to a reasonable estimate of how rapidly the atmosphere would cool if the sun were suddenly removed. For example, as the Earth rotates from daytime to nighttime, half the atmosphere is in the dark. If the sun were suddenly "turned off" in the window-gray model, the atmospheric

temperature would be given by

$$mC_P \frac{dT_A}{dt} = \varepsilon\sigma T_S^4 - 2\varepsilon\sigma T_A^4 \tag{1.22}$$

with $m = 1.034 \times 10^4\ \mathrm{kg\,m^{-2}}$ the mass per unit area for the atmosphere. If the heat capacity of the surface is zero, then without the sun, the surface energy budget is given by

$$\sigma T_S^4 = \varepsilon\sigma T_A^4 \tag{1.23}$$

Note that without the sun the surface is colder than the atmosphere, as it often is on a cloud-free night when the absolute humidity is relatively low. Such conditions are common to high latitude continental regions during winter. Without the sun, the surface is heated by the atmosphere. Combining Equations 1.22 and 1.23, the temperature of the atmosphere is given by

$$mC_P \frac{dT_A}{dt} = -\varepsilon(2-\varepsilon)\sigma T_A^4 \tag{1.24}$$

As expected, the atmospheric temperature will decrease once the sun is removed. The initial temperature trend is obtained by expanding the atmospheric temperature into a constant equilibrium temperature T_{A0} and a perturbation temperature $T' \ll T_{A0}$. The expansion gives

$$mC_P \frac{dT'}{dt} = -\varepsilon(2-\varepsilon)\sigma T_{A0}^4 - 4\varepsilon(2-\varepsilon)\sigma T_{A0}^4 \frac{T'}{T_{A0}} \tag{1.25}$$

Rearranging the terms yields

$$\frac{dT'}{dt} + \frac{T'}{\tau} = -\frac{\varepsilon(2-\varepsilon)\sigma T_{A0}^4}{mC_P} \tag{1.26}$$

with the radiative time constant for the atmosphere given by

$$\tau = \frac{mC_P T_{A0}}{4\varepsilon(2-\varepsilon)\sigma T_{A0}^4} \tag{1.27}$$

Using values derived for the window-gray model, $\tau = 39$ days, about a month. This value is close to the radiative time constant estimated for the Earth's atmosphere.

Multiplying Equation 1.26 by the integration factor $e^{t/\tau}$ gives

$$e^{\frac{t}{\tau}} dT' + \frac{T'}{\tau} e^{\frac{t}{\tau}} dt = -\frac{\varepsilon(2-\varepsilon)\sigma T_{A0}^4}{mC_P} e^{\frac{t}{\tau}} dt \tag{1.28}$$

The integration factor together with the chain rule for differentiation transforms Equation 1.28 to give

$$d\left(T' e^{\frac{t}{\tau}}\right) = -\frac{\varepsilon(2-\varepsilon)\sigma T_{A0}^4}{mC_P} e^{\frac{t}{\tau}} dt \tag{1.29}$$

Integrating both sides of Equation 1.29 from time $t = 0$, when $T' = 0$, to some arbitrary time t yields the perturbation temperature at time t given by

$$T'(t) = -\frac{\varepsilon(2-\varepsilon)\sigma T_{A0}^4}{mC_P}\int_0^t dt' e^{\frac{t'-t}{\tau}} \tag{1.30}$$

Performing the integration produces

$$T'(t) = -\tau\frac{\varepsilon(2-\varepsilon)\sigma T_{A0}^4}{mC_P}\left(1-e^{-\frac{t}{\tau}}\right) = -\frac{T_{A0}}{4}\left(1-e^{-\frac{t}{\tau}}\right) \tag{1.31}$$

Since the atmosphere spends half a day turned away from the sun, and since for half a day, $t \ll \tau$, the nighttime temperature change is approximately given by

$$T'(t) = -\frac{T_{A0}}{4}\frac{t}{\tau} = -\frac{242}{4\times 2\times 39}\,\mathrm{K} = -0.8\,\mathrm{K} \tag{1.32}$$

There is indeed little difference, about 1 K between the daytime and nighttime average temperature of the Earth's atmosphere. Of course, on the ground, under stable weather conditions in a dry climate, one can experience large swings in air temperature. Under such conditions, however, most of the change is confined to the boundary layer, typically the lowest 100 hPa or so. The temperature of the rest of the atmospheric column hardly changes.

1.7 Composition of the Earth's Atmosphere

The absorption and emission of radiation in the Earth's atmosphere shapes the vertical structure of the global average atmospheric temperature profile. The absorption and emission depend on the concentrations of the gases and particles that absorb and emit the radiation. Table 1.1 lists the concentrations and approximate atmospheric residence times for the major gases. Gases such as nitrogen and

Table 1.1 Concentrations and approximate residence times of gases in the Earth's atmosphere.

Gas	Concentration	Approximate residence time
Nitrogen, N_2	78%	N/A
Oxygen, O_2	21%	N/A
Argon, Ar	1%	N/A
Water vapor, H_2O	0–2%	1 wk
Carbon dioxide, CO_2	390 ppmv	100 yr
Ozone, O_3	0–500 ppbv	1–150 d
Methane, CH_4	1750 ppbv	10 yr
Nitrous oxide, N_2O	300 ppbv	150 yr
CFCs	1 ppbv	100 yr

oxygen make up such large fractions of the atmosphere that changes in their concentrations from, for example, combustion, oxidation, and nitrogen fixation, are negligibly small. Gases with residence times greater than about a decade are considered to be long-lived. Through the mixing and circulation of the atmosphere, these gases have concentrations that are constant. Their concentrations remain unchanged within a small percentage relative to nitrogen and oxygen, throughout the Earth's atmosphere from the surface to the stratopause (altitude ~50 km) and beyond.

Gases with short residence times, such as water vapor and ozone, have high concentrations near their sources and low concentrations near their sinks. The source for water vapor is evaporation and evapotranspiration at the surface. The global average concentration of water vapor held in a column of air is approximately 2 g cm^{-2}, or equivalently 2 cm of precipitable water. Precipitable water is the depth to which a layer of water would cover the Earth's surface if all of the water vapor in the atmosphere were condensed into liquid. Evaporation is high where surface temperatures are high, as in the tropics, and low where temperatures are low, as at high latitudes. Within latitude belts, the zonal average concentration of water vapor in the atmosphere follows that of the average surface temperature and an average surface relative humidity near 80%. Since temperature generally falls with altitude in the troposphere, the condensation of water vapor in the atmosphere increases with altitude and water vapor is depleted through precipitation. Figure 1.3 shows the normalized pressure of the atmosphere as a function of altitude along with the normalized vapor pressure for water. The global average scale height of the atmosphere is about 8 km. The scale height gives the exponential rate of decrease in pressure with altitude. With a scale height of 8 km, atmospheric pressure is halved every 5 km. Water vapor has a scale height of about 2 km. Vapor pressure is halved about every 1.5 km. The decrease in the concentration of water

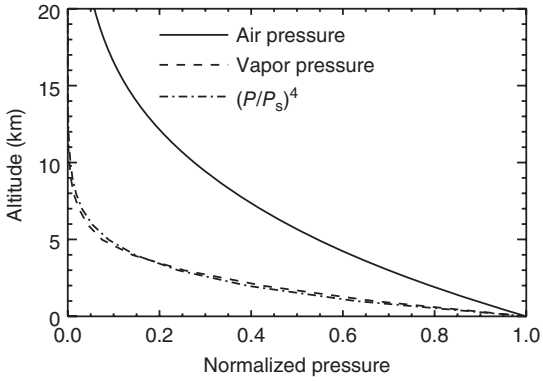

Figure 1.3 Normalized air pressure (solid line) and water vapor pressure (dashed line). The normalized pressures are the pressure divided by the surface value. The dashed dotted line gives the normalized vapor pressure for water when the mass mixing ratio is given by Equation 1.36b.

vapor with altitude approximately follows the decrease of temperature with altitude and a relative humidity that decreases linearly with pressure from the surface to the tropopause [7]. The tropopause is the demarcation between the troposphere and stratosphere. The altitude of the tropopause ranges from as high as 18 km near the equator to as low as 10 km in the polar regions.

The ratio of the scale heights for atmospheric pressure (8 km) and that for water vapor pressure (2 km) suggests that water vapor pressure at pressure level P, $p_{\mathrm{VAP}}(P)$, normalized by its value at the surface $p_{\mathrm{VAP\,S}}$, can be approximated by

$$\frac{p_{\mathrm{VAP}}(P)}{p_{\mathrm{VAP\,S}}} = \left(\frac{P}{P_{\mathrm{S}}}\right)^4 \tag{1.33}$$

with P_{S} the surface pressure. As indicated by the dash–dotted curve in Figure 1.3, the simple power law in Equation 1.33 matches closely the climatological profile of the normalized water vapor pressure.

The mass mixing ratio of a gas is the ratio of the density of the gas to that of the air that contains the gas. In this book, mass mixing ratio is expressed as the mass of a gas divided by the mass of dry air that contains the gas. The water vapor pressure is given by the ideal gas law

$$p_{\mathrm{VAP}}(P) = \rho_{\mathrm{VAP}}(P) R_{\mathrm{H_2O}} T(P) \tag{1.34}$$

with $R_{\mathrm{H_2O}}$ the gas constant for water vapor. It is related to the gas constant for dry air through the universal gas constant R^* by

$$R_{\mathrm{H_2O}} = \frac{R^*}{m_{\mathrm{H_2O}}} = \frac{R^*}{m_{\mathrm{AIR}}} \frac{m_{\mathrm{AIR}}}{m_{\mathrm{H_2O}}} = R_{\mathrm{AIR}} \frac{m_{\mathrm{AIR}}}{m_{\mathrm{H_2O}}} \tag{1.35}$$

with $m_{\mathrm{AIR}} = 0.029\,\mathrm{kg}$ the molar weight of dry air and $m_{\mathrm{H_2O}} = 0.018\,\mathrm{kg}$ the molar weight of water vapor. In terms of the mass mixing ratio, Equation 1.34 is given by

$$p_{\mathrm{VAP}}(P) = r(P) \rho_{\mathrm{AIR}}(P) R_{\mathrm{AIR}} \frac{m_{\mathrm{AIR}}}{m_{\mathrm{H_2O}}} T(P) = r(P) \frac{m_{\mathrm{AIR}}}{m_{\mathrm{H_2O}}} P \tag{1.36a}$$

so that

$$r(P) = r_{\mathrm{S}} \left(\frac{P}{P_{\mathrm{S}}}\right)^3 \tag{1.36b}$$

with $r_{\mathrm{S}} = r(P_{\mathrm{S}})$ the mass mixing ratio at the surface.

Turning to ozone, some is created in the lower atmosphere through photochemical reactions with oxides of nitrogen in the presence of hydrocarbons. Ozone, being highly reactive, is removed from the lower atmosphere through the oxidation of trace gases and contact with surfaces. Most of the atmospheric ozone is produced in the tropical stratosphere where ultraviolet radiation (UV) photodissociates oxygen molecules. Odd oxygen atoms from the split molecules combine with other molecules of oxygen to form ozone. At altitudes in the stratosphere where its concentration peaks, ozone is removed through catalytic reactions, mostly those involving oxides of nitrogen. Ozone is also photodissociated by UV radiation. The photodissociation of ozone prevents harmful UV

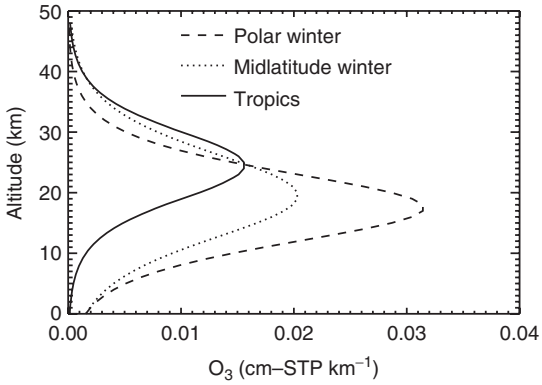

Figure 1.4 Concentrations of ozone derived from Equation 1.37. Values of the parameters are given in Table 1.2.

Table 1.2 Parameters used in Equation 1.37 to determine the concentration of ozone shown in Figure 1.4.

Profile	*a* (cm-STP)	*b* (km)	*c* (km)
Tropics	0.25	25	4
Midlatitude winter	0.4	20	5
Polar winter	0.5	18	4

Parameters from Lacis and Hansen [9].

from reaching the surface, making the stratospheric ozone layer the protective shield for the Earth's biosphere. Figure 1.4 shows vertical profiles for the tropics, midlatitude winters, and polar winters. The profiles are based on analytic fits to observations [8]. The amount of ozone above a given altitude z is given by

$$u(z) = \frac{a[1 + \exp(-b/c)]}{1 + \exp((z - b)/c)} \tag{1.37}$$

with a the total amount of ozone in the atmospheric column, b the altitude at which the ozone concentration peaks, and c the scale height for ozone above the altitude at which the concentration peaks. Table 1.2 gives the values of the parameters used to produce the concentrations shown in Figure 1.4. The concentration of ozone derived from Equation 1.37 has units of density, cm-STP/km, with STP (standard temperature and pressure) 273.15 K and 1 atm = 1013.25 hPa.

The unit cm-STP used above to specify the column amounts of ozone is the gaseous analog of precipitable cm used to express the column amount of water vapor in terms of an equivalent amount of liquid water. If all the ozone in the atmosphere was reduced to STP, it would cover the surface of the Earth with a layer that is so many cm-STP thick. The column amount a in Equation 1.37 is typically between 0.2 and 0.5 cm-STP. A very thin layer of ozone protects the biosphere

from UV. To translate cm-STP to other units, recall that 6.022×10^{23} molecules (1 mole) occupy a volume of 22.4×10^3 cm^3 at STP. Column amounts of 1 cm-STP and 2.69×10^{23} molecules m^{-2} are equivalent. As an exercise, the reader may show that the atmospheric scale height, 8 km, is the depth of the atmosphere when reduced to STP.

While ozone is generated primarily in the tropical stratosphere, its column concentration is the smallest in the tropics. The ozone that is produced in the tropical stratosphere is transported downwards and polewards in both hemispheres by a stratospheric circulation. Ozone piles up at higher latitudes, especially during the polar winters, where the amount of UV radiation needed for the ozone depleting reactions is low compared with its amount in the tropics.

Carbon dioxide has a constant concentration throughout the atmosphere. Its mass mixing ratio is 5.92×10^{-4} g CO_2/g AIR. A volume mixing ratio is the number of molecules of a trace gas to the number of air molecules that contains the gas. For carbon dioxide in the Earth's atmosphere the equivalent volume mixing ratio as of 2010 is 390 ppmv (parts per million by volume).

Finally, aerosols are composed of small particles in the atmosphere. The particles scatter sunlight and make skies look "hazy." Aerosol particles are often referred to as *haze particles* or simply "haze." Similarly to water vapor, aerosols have residence times in the atmosphere of a few days to perhaps a week or so depending on the altitudes to which they can be lofted, primarily through convective updrafts. Some aerosol particles are generated near the surface by combustion and by mechanical lofting. They arise from both human and natural sources, from the burning of fossil fuels, forest fires, windblown dust, and sea spray. Aerosol particles can also have precursors, gases injected into the atmosphere, which through photochemical reactions give rise to particles. Aerosols congregate near their sources and their concentrations diminish with distance from their sources. Particles are removed through settling, deposition on surfaces, and washout by precipitation. Particles from intense forest fires and desert wind storms can be lofted to middle and upper tropospheric levels. Layers of particles at those altitudes have been observed to traverse both the Atlantic and Pacific oceans. Aerosols are known to absorb and reflect a significant amount of sunlight, 1–2%. Their effects on sunlight are often visible as the cause of reduced visibility, a whitening of the blue sky, and a reddening of sunsets. Owing to their relatively short lifetimes, however, their properties and concentrations are highly variable in both space and time. This variability makes their effects on the Earth's energy budget difficult to assess.

Gases in the atmosphere contribute to the Rayleigh scattering of incident sunlight. This type of scattering causes cloud-free skies under relatively aerosol-free conditions to be blue. On the other hand, only a few gases absorb significant amounts of light. As discussed in later chapters, strong absorbers such as water vapor, ozone, and nitrous oxide have permanent electric dipole moments. These dipole moments arise from the asymmetric structures of the molecules coupled with the congregation of electrons around certain atoms within the molecule balanced by the loss of electrons around other atoms. The oscillations of the resulting dipole moments through the vibrations of the atomic bonds and the

rotation of the molecules result in strong interactions with radiation, particularly at infrared and microwave wavelengths. Diatomic molecules, such as nitrogen and oxygen, have no permanent electric dipole moments and consequently interact only weakly with radiation. Oxygen molecules undergo electronic transitions creating a magnetic dipole moment and weak absorption (~2%) of sunlight at visible wavelengths. Symmetrical molecules, such as carbon dioxide and methane, lack permanent electric dipole moments but they attain the required oscillating electric dipole moments when the bonds between the atoms vibrate and bend. The vibrations and bending of the bonds and the rotation of these molecules lead to strong interactions with radiation.

1.8
Radiation and the Earth's Mean Temperature Profile

If the single-layer, window-gray atmosphere is replaced with two isothermal but different layers, radiative equilibrium requires that the temperature of the lower atmospheric layer be higher and that of the higher atmospheric layer be lower than the atmospheric temperature of the single-layer model. Thus, in the two-layer, window-gray, radiative equilibrium model, as in the Earth's atmosphere, the temperature decreases with altitude. The proof is left to the reader.

Of course, the atmosphere is far more complex than a two-layer system. A simple approach for the temperature profile in a window-gray, radiative equilibrium model is feasible using an approximate solution for the equation of radiative transfer [10, 11]. In this simple solution, the temperature of the atmosphere falls with altitude from the surface until becoming isothermal in the upper regions of the atmosphere. The isothermal layer at the top of the atmosphere has a temperature given by $T_{\mathrm{ISO}} = T_e/2^{1/4} = 214\,\mathrm{K}$. This solution was first obtained by Karl Schwarzschild in the early 1900s. It followed balloon-borne measurements around the turn of the twentieth century that had reached altitudes near the tropopause, thereby revealing the existence of a stratosphere. The temperature of the isothermal top layer obtained with the window-gray model was close to those observed at the base of the stratosphere.

In radiative equilibrium, the radiative energy absorbed within each layer of the atmosphere is equal to the radiation emitted. In the case of the single-layer, window-gray model, this equilibrium is given by

$$mC_P \frac{dT_{\mathrm{A}}}{dt} = \left[\frac{Q_0}{4}(1-\alpha) - (1-\varepsilon)\sigma T_{\mathrm{S}}^4 - \varepsilon\sigma T_{\mathrm{A}}^4\right] - \left[\frac{Q_0}{4}(1-\alpha) + \varepsilon\sigma T_{\mathrm{A}}^4 - \sigma T_{\mathrm{S}}^4\right] \tag{1.38}$$

The first term in brackets on the right-hand side is recognized as the radiation budget at the top of the atmosphere. It is the sunlight absorbed by the Earth's atmosphere-surface system minus the infrared radiation emitted by the system. Notice that both the solar and emitted infrared radiation can be broken into upward and downward solar and infrared radiation fluxes. Radiative fluxes have

units of power per unit area (W m^{-2}) and are defined in terms of the properties of light in Chapter 2. The upward solar radiative flux is the reflected sunlight given by

$$Q^{+}_{\mathrm{TOP}} = \alpha Q_0/4 \tag{1.39a}$$

and the downward flux is the incident sunlight given by

$$Q^{-}_{\mathrm{TOP}} = Q_0/4 \tag{1.39b}$$

In atmospheric radiation the upward direction is indicated by a "+" sign and the downward direction by a "−" sign. The net solar radiative flux is the upward flux minus the downward flux, $Q_{\mathrm{NET\,TOP}} = Q^{+}_{\mathrm{TOP}} - Q^{-}_{\mathrm{TOP}}$. Similarly, the upward radiation emitted at the top of the atmosphere is given by

$$F^{+}_{\mathrm{TOP}} = (1-\varepsilon)\sigma T^4_{\mathrm{S}} + \varepsilon\sigma T^4_{\mathrm{A}} \tag{1.40a}$$

the sum of the radiation emitted by the Earth's surface and transmitted by the atmosphere and the radiation emitted by the atmosphere. The downward infrared flux at the top of the atmosphere is zero:

$$F^{-}_{\mathrm{TOP}} = 0 \tag{1.40b}$$

The net infrared radiative flux at the top of the atmosphere, similarly to the net solar radiative flux, is given by the difference $F_{\mathrm{NET\,TOP}} = F^{+}_{\mathrm{TOP}} - F^{-}_{\mathrm{TOP}}$. Consequently, at the top of the atmosphere, the Earth's radiation budget is given in terms of the net radiative flux by

$$\begin{aligned}\mathscr{R}_{\mathrm{NET\,TOP}} &= -\mathscr{F}_{\mathrm{NET\,TOP}} = -[Q^{+}_{\mathrm{TOP}} - Q^{-}_{\mathrm{TOP}} + F^{+}_{\mathrm{TOP}} - F^{-}_{\mathrm{TOP}}] \\ &= -(Q_{\mathrm{NET\,TOP}} + F_{\mathrm{NET\,TOP}})\end{aligned} \tag{1.41}$$

with $\mathscr{F}_{\mathrm{NET\,TOP}}$ the total net radiative flux, the sum of the solar net radiative flux and the net emitted radiative flux at the top of the atmosphere.

The second term in brackets in Equation 1.38 is the net radiation budget for the Earth's surface. In the window-gray model, the net solar radiative flux at the surface is the same as that at the top of the atmosphere. The net infrared flux is given by

$$F_{\mathrm{NET\,SURF}} = F^{+}_{\mathrm{SURF}} - F^{-}_{\mathrm{SURF}} = \sigma T^4_{\mathrm{S}} - \varepsilon\sigma T^4_{\mathrm{A}} \tag{1.42}$$

As with the top of the atmosphere, the radiation budget at the surface is related to the net radiative flux by $\mathscr{R}_{\mathrm{NET\,SURF}} = -\mathscr{F}_{\mathrm{NET\,SURF}}$.

Combining the terms in Equation 1.38, the rate of change of the atmospheric temperature is given by

$$mC_P\frac{dT_{\mathrm{A}}}{dt} = -(\mathscr{F}_{\mathrm{NET\,TOP}} - \mathscr{F}_{\mathrm{NET\,SURF}}) = \varepsilon\sigma T^4_{\mathrm{S}} - 2\varepsilon\sigma T^4_{\mathrm{A}} \tag{1.43}$$

As has already been noted, in the window-gray model the atmosphere is heated by the absorption of infrared radiation emitted by the surface and cooled by the emission of infrared radiation by the atmosphere. In radiative equilibrium, the cooling balances the heating and the net is zero. The temperature remains constant.

Consider, however, the rapid increase in the Earth's albedo after the Mt. Pinatubo eruption. The sunlight absorbed by the Earth decreased while the emitted infrared radiation at the top of the atmosphere remained largely unchanged. The Earth began to cool. In the window-gray, radiative equilibrium model, the surface has no heat capacity. The surface temperature decreases as the albedo increases. Owing to its heat capacity, on the other hand, the atmosphere does not immediately change its temperature. The temperature decreases with time until a new equilibrium is reached. With no heat capacity, the surface temperature is forced to maintain radiative equilibrium. As a result, the surface temperature initially drops but then slowly decreases in response to the decreasing atmospheric temperature. Ultimately, a new equilibrium is reached so that emission by the surface and emission by the atmosphere–surface system balance the radiation that each absorbs.

If a greenhouse gas in the atmosphere were to suddenly increase, the absorption of infrared radiation by the gas would cause the emission at the top of the atmosphere to suddenly decrease. For a greenhouse gas that does not absorb sunlight, the amount of sunlight absorbed would remain unchanged. The Earth would warm. At the surface, owing to the increase in the greenhouse gas, the emission downward by the atmosphere at the surface would increase, thereby increasing the absorption of emitted radiation by the surface. The surface temperature would rise so that the rate of emission by the surface balanced the rate of absorption by the surface, the sum of the rates for the absorption of sunlight and the infrared radiation emitted downwards by the atmosphere. The temperature of the atmosphere would also rise partly because of the increase in absorption from the increase in the greenhouse gas concentration and partly because of the increase in radiation emitted by the surface that the atmosphere absorbs. The rate of rise in temperature would be moderated by the heat capacity of the atmosphere. Ultimately, the atmospheric temperature would rise until a new state of radiative equilibrium is reached. At its new equilibrium temperature, the rate at which the atmosphere absorbs infrared radiation would match the sum of the rates at which it emits upward to space and downward to the surface. Similarly, at its new equilibrium temperature, the rate at which the surface absorbs sunlight and infrared radiation emitted downwards by the atmosphere would match the rate at which it emits infrared radiation.

Within a multilayered atmosphere, the radiative heating of a layer of thickness Δz is, from Equation 1.43, given in terms of the vertical gradient of the total net radiative flux,

$$\frac{dT}{dt} = -\frac{1}{\rho(z)C_P}\frac{\Delta \mathscr{F}_{\mathrm{NET}}}{\Delta z} \tag{1.44}$$

with $\rho(z)\Delta z$ the mass of the layer. In Equation 1.44, $-\Delta \mathscr{F}_{\mathrm{NET}}/\Delta z = \Delta \mathscr{R}_{\mathrm{NET}}/\Delta z$ is the change in the net radiation budget of the layer. It is the change in the rate at which the layer absorbs radiation minus the change in the rate at which the layer emits radiation. For infinitesimally thin layers, the radiative

heating rate is given by

$$\frac{dT}{dt} = -\frac{1}{C_P \rho(z)} \frac{d\mathcal{F}_{\mathrm{NET}}}{dz} \tag{1.45a}$$

or equivalently after applying hydrostatic balance by

$$\frac{dT}{dt} = \frac{g}{C_P} \frac{d\mathcal{F}_{\mathrm{NET}}}{dP} \tag{1.45b}$$

For a multilayered atmosphere in radiative equilibrium, the rate of absorption by each layer equals the rate of emission. The rate of absorption is the sum of the rates for the sunlight and emitted radiation absorbed by the layer. The emitted radiation incident on the layer is the radiation emitted downward by layers above the layer and transmitted by the intervening atmosphere to the layer. The radiation is combined with radiation emitted upwards by layers below the layer and emitted by the surface that is transmitted to the layer by the intervening atmosphere. If, for example, an aerosol layer forms in the stratosphere after a volcanic eruption, the rate of sunlight absorbed by the layer decreases and the layer would cool until equilibrium is reached between the rate it absorbs radiation and the rate it emits. Conversely, if the concentration of an infrared absorber in a layer increases, the layer would warm until equilibrium is reached between the absorption and emission of infrared radiation.

Unfortunately, calculating the effects of heating in a multilayered, nongray, nonisothermal atmosphere is a formidable undertaking. Figure 1.5 shows the results of early attempts to obtain realistic solutions for the vertical temperature profile of the Earth's atmosphere in radiative equilibrium [6]. The temperatures at the centers of the model layers are indicated by the large dots in the figure. In these early attempts, the composition of the atmosphere was taken to be close to the global average conditions of the 1960s. The concentrations of gases then differed from those presented in Section 1.7 only for the greenhouse gases that have increased as a result of human activity. Initially, the atmosphere in the model was assumed to be cloud-free. In radiative equilibrium, the Earth's atmospheric temperature under cloud-free conditions decreased rapidly from a surface temperature of over 330 K to a temperature of 190 K at 10 km, a temperature gradient of $-14\,\mathrm{K\,km^{-1}}$.

A vertical temperature gradient of $-14\,\mathrm{K\,km^{-1}}$ is unsustainable in the Earth's atmosphere. Such conditions are buoyantly unstable. The temperature of a gas cannot decrease faster than the rate given by the vertical temperature gradient associated with adiabatic processes. This temperature gradient is referred to as the *adiabatic lapse rate*. If the temperature decreases more rapidly with increasing altitude than that given by the adiabatic lapse rate, then a parcel of air experiencing a small vertical displacement would either rocket upwards or plunge downwards, depending on the initial direction of its displacement. Unstable temperature gradients create rapid vertical motions referred to as *convection*, which, through the mixing of air, reshapes the temperature profile so that it becomes buoyantly stable. As long as the decrease of temperature with altitude is less than that given by the adiabatic lapse rate, small vertical displacements of an air parcel will lead to

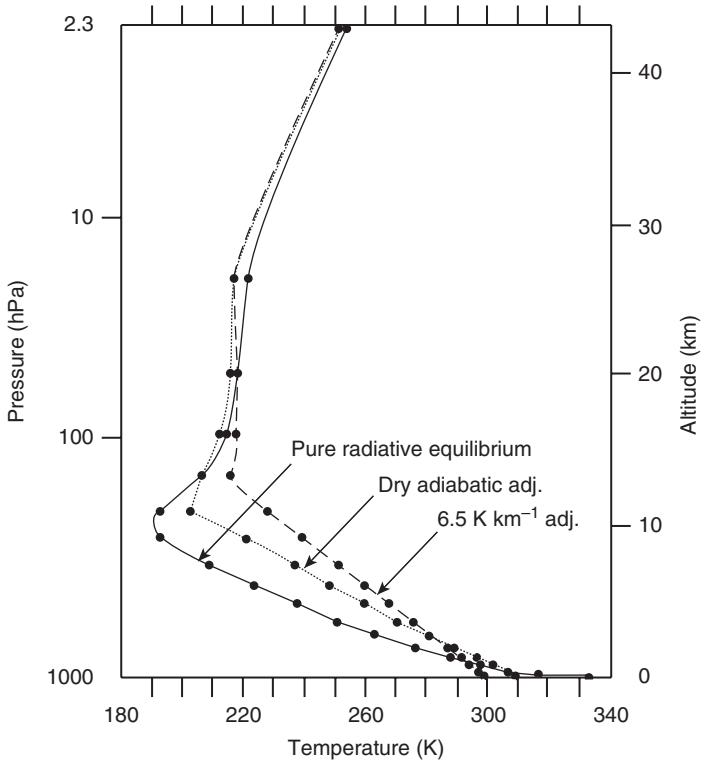

Figure 1.5 Temperature profiles for global average abundances of water vapor, carbon dioxide, and ozone. The profiles were calculated for cloud-free conditions by Manabe and Strickler [6]. The solid curve is for radiative equilibrium. Curves for the cases in which the critical lapse rate was taken to be equal to the dry adiabatic lapse rate (dashed) and 6.5 K km^{-1} (dotted) are also shown. (After Manabe and Strickler [6]. Reproduced by permission of the American Meteorological Society.)

restoring forces that return the parcel to its original altitude. Barring the passage of weather fronts, temperature profiles satisfying buoyantly stable conditions can exist indefinitely. The stratosphere, for example, was so named because its temperature gradient ranges from near zero near the tropopause to positives values at higher altitudes. The stratosphere is thus stably stratified.

The adiabatic lapse rate is derived from the conservation of energy and the relationship for hydrostatic balance. Assuming negligible vertical motion, the hydrostatic balance is between the pull of gravity on a volume of air and the change in pressure with altitude, which holds the mass in place. For adiabatic processes, $dQ = 0$. With hydrostatic balance, conservation of energy as given by Equation 1.2 for adiabatic processes leads to

$$C_p \frac{dT}{dz} = \frac{1}{\rho} \frac{dP}{dz} = -g \tag{1.46}$$

The adiabatic lapse rate is given by

$$\Gamma = -\frac{dT}{dz} = \frac{g}{C_p} \tag{1.47}$$

The temperature lapse rate is the decrease in temperature with altitude. A positive lapse rate indicates decreasing temperature with altitude. For the Earth, $g = 9.8\,\mathrm{m\,s^{-2}}$ giving $\Gamma = 9.8\,\mathrm{K\,km^{-1}}$. This lapse rate is referred to as the *dry adiabatic* lapse rate because it does not account for the heating of air due to the release of latent heat as water vapor condenses. The release of latent heat raises the surrounding air temperature, leading to a smaller lapse rate, less negative vertical temperature gradient. For saturated air, the lapse rate is referred to as the *moist adiabatic* lapse rate. With the effects of radiation, release of latent heat, and other dynamical processes, the lapse rate for the Earth's atmosphere ranges from about $4\,\mathrm{K\,km^{-1}}$ for moist tropical air to $9.8\,\mathrm{K\,km^{-1}}$ for dry desert air.

In radiative equilibrium, the composition of the Earth's atmosphere produces a buoyantly unstable vertical temperature profile throughout most of the troposphere as shown in Figure 1.5. A temperature profile that is close to the average profile of the northern hemisphere is obtained when the observed lapse rate for the northern hemisphere, $6.5\,\mathrm{K\,km^{-1}}$, is taken to be the "critical lapse rate." The critical lapse rate distinguishes "buoyantly unstable" layers from stable layers. When the radiative equilibrium solution produces a supercritical lapse rate between model layers, the temperatures of the layers are adjusted so that the difference between the layers is given by the critical lapse rate. This procedure is called *convective adjustment*. The combination of radiative equilibrium and convective adjustment leads to "radiative–convective equilibrium."

Figure 1.6 shows the resulting net radiative heating rates for radiative–convective equilibrium. Forcing the temperature lapse rate to a critical value whenever the radiative equilibrium lapse rate becomes supercritical leads to a troposphere that is radiatively cooling. In radiative–convective equilibrium, the lapse rate is assumed to maintain a critical value through an unspecified combination of radiative, convective, and latent heating.

The troposphere is approximately 80% of the atmosphere. Its radiative cooling rate is about 1 K/day. For global average conditions, large-scale dynamical processes produce no net heating of the atmosphere. Most of the radiative cooling by the atmosphere is compensated by heating due to the release of latent heat when water vapor condenses, freezes, and falls as precipitation. The surface also is not in radiative equilibrium, but must lose energy to the atmosphere, which it does, through turbulent exchange (dry sensible heat), evaporation, and evapotranspiration (latent heat) as shown in Figure 1.7. Much of this heat is transferred through convective processes.

Figure 1.7 depicts an approximate breakdown of the heating and cooling for the surface, troposphere, and stratosphere. The data are taken from Hartmann [12]. The values in the figure are expressed as percentages of the incident global average sunlight. The figure depicts the Earth and the stratosphere as being in balance, consistent with the radiative heating rates for radiative–convective equilibrium

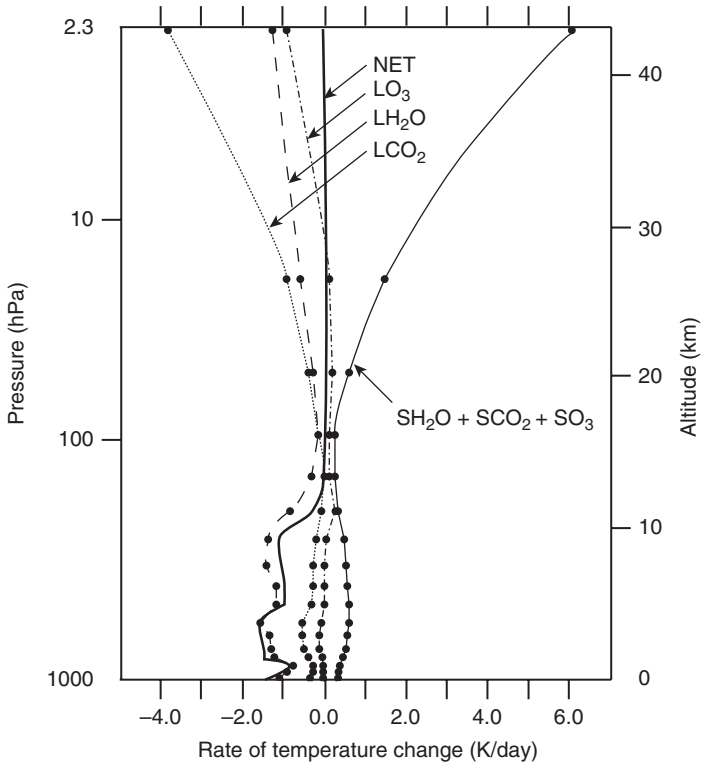

Figure 1.6 Radiative heating rates due to absorption of sunlight under average cloudy conditions, $SH_2O + SCO_2 + SO_3$, and absorption and emission of infrared radiation, LH_2O, LO_3, and LCO_2. The "S" indicates solar heating rates and the "L" indicates longwave heating and cooling rates. The solid curve labeled NET is the net radiative heating rate. In the stratosphere, it is zero. (After Manabe and Strickler [6]. Reproduced by permission of the American Meteorological Society.)

shown in Figure 1.6. At the tropopause, the troposphere and surface together are also in radiative equilibrium. The sunlight absorbed by the troposphere and Earth's surface balances the net infrared radiation emitted upward at the tropopause. The figure identifies the primary contributors of absorption and emission in the atmosphere.

The spectra of the incident and transmitted sunlight and the emitted radiation at the top of the atmosphere coupled with the absorption spectra of the molecules that account for the absorption lead to the identification of the major contributors in Figure 1.7. Figure 1.8a shows calculated spectra for the incident sunlight at the top of the atmosphere and at the surface when cloud-free and when overcast by cirrus. The profiles of water vapor, carbon dioxide, and ozone in these calculations are those of the U.S. Standard Atmosphere. These profiles are close to global, annual average profiles described in Section 1.7. The surface albedo for these calculated spectra is 0.1. The visible optical thickness of the cirrus is 2. Chapter 3

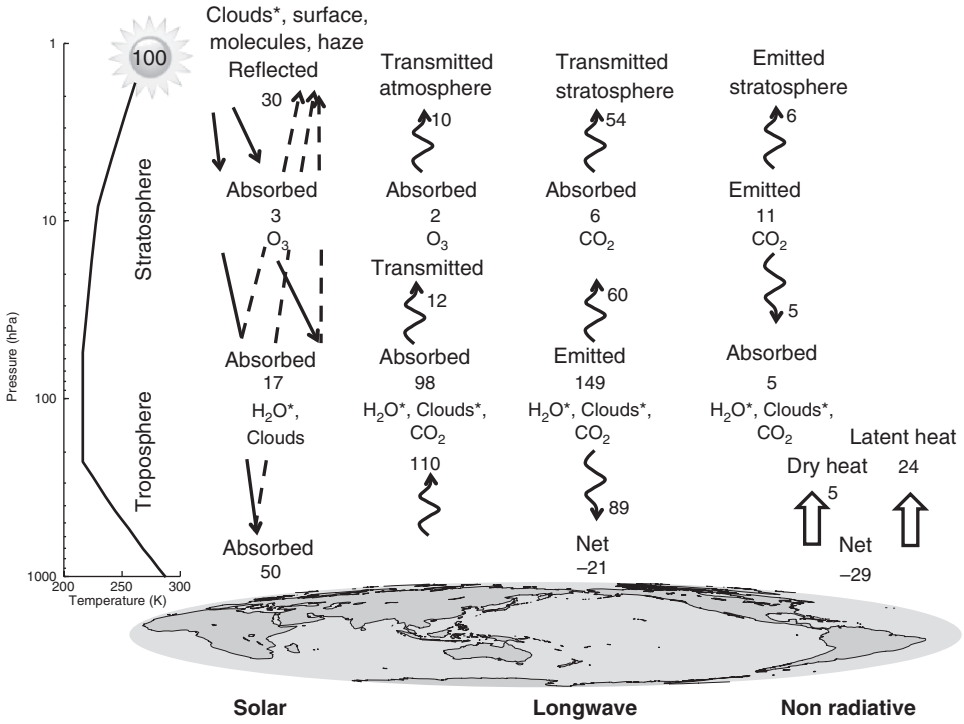

Figure 1.7 Global average energy budget of the surface, troposphere, and stratosphere. (Data are taken from Hartmann [12].) Asterisks indicate the major radiatively active contributors to the absorption and scattering of sunlight and the absorption and emission of thermal radiation. The values are given as a percentage of the global average incident sunlight, $Q_0/4 = 340\,\mathrm{W\,m^{-2}} \equiv 100\%$. The temperature at left is the 1976 U.S. Standard Atmosphere profile.

describes the interaction of radiation with matter, which leads to the definition of optical thickness. With a visible optical thickness of 2, the cirrus is relatively thick but not uncommonly so. The cirrus is sufficiently thick to whiten the sky but not so thick that it prevents the sun's disk from being clearly seen through the cloud by a surface observer. The effective size of the ice crystals used in the calculation is 50 μm, a typical value. In fact, the cirrus optical properties were those used to retrieve visible optical depths and particle sizes from multispectral imagery of reflected sunlight and emitted infrared radiation collected by NASA's satellite-borne Moderate Resolution Imaging Spectroradiometer (MODIS) [13]. The spectral distribution of radiation emitted by a blackbody with a temperature of 5800 K is also shown in Figure 1.8a. The distribution represents fairly well the spectral variation of the incident sunlight. Chapter 2 describes blackbody radiation.

Figure 1.8a identifies the major molecular absorption bands for the downward solar radiation at the surface. Chapter 5 describes molecular absorption bands. Chapter 6 applies the principles described in Chapters 2–5 to account for the

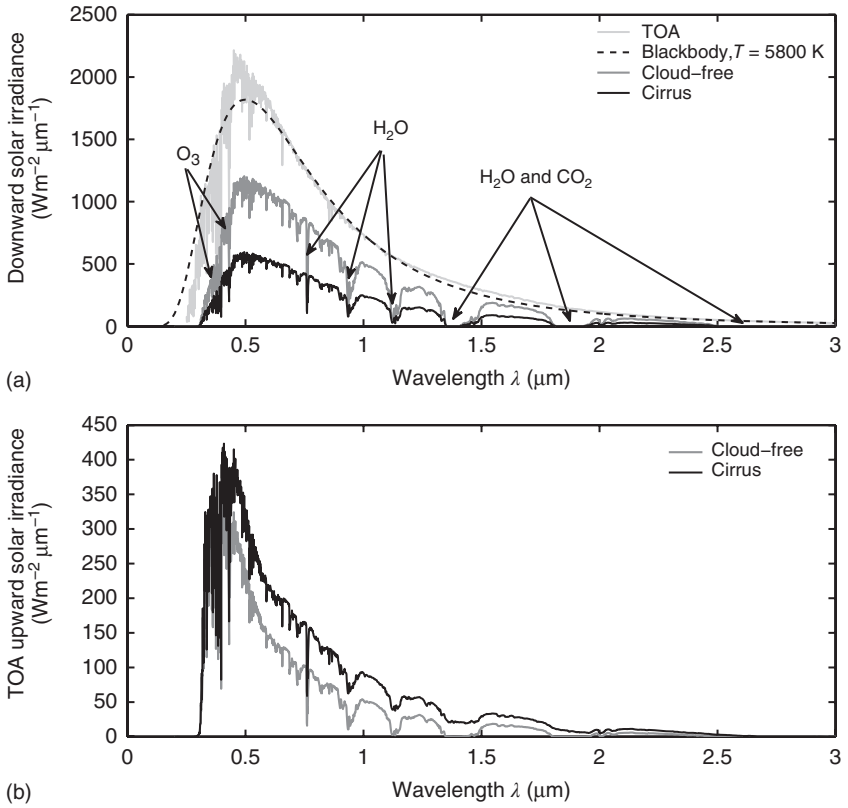

Figure 1.8 Simulated incident solar radiation at the top of the atmosphere (TOA) and at the surface under cloud-free and cirrus conditions (a) and reflected sunlight at the top of the atmosphere (b). The surface albedo in the calculations is 0.1 and the solar zenith angle is 45°. The atmospheric composition and temperature profile are those of the U.S. Standard Atmosphere. The cirrus cloud lies between 9 and 10 km, has a visible optical depth of 2, and an effective particle size of 50 μm. Also shown in (a) is the spectral distribution of radiation emitted by a blackbody at a temperature of 5800 K.

absorption and scattering of sunlight by the Earth's atmosphere and surface. The chapter describes how ozone absorbs nearly all of the incident radiation at wavelengths less than 0.3 μm, accounting for the absorption of nearly 2% of the incident sunlight. Ozone also absorbs relatively weakly over the entire range of the visible spectrum 0.4–0.7 μm, accounting for the absorption of another 1% of the incident sunlight. Water vapor absorbs a substantial fraction of the sunlight at wavelengths in the near infrared, wavelengths ranging from 0.7 μm to less than about 5 μm.

Figure 1.8b shows the reflected solar spectra at the top of the atmosphere under cloud-free and the same cirrus conditions used for Figure 1.8a. Clearly, the cirrus adds considerably to the reflected sunlight even though the cloud is not so thick as to block the solar disk from being viewed from the surface.

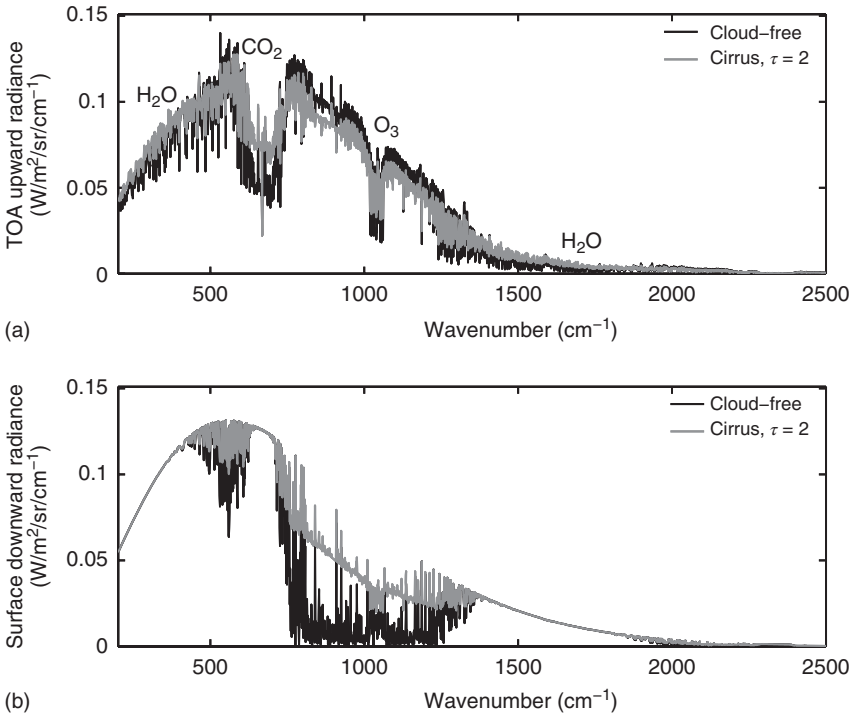

Figure 1.9 Simulated emitted radiation at the top of the atmosphere (a) and radiation emitted downward by the atmosphere at the surface (b) for cloud-free and cirrus conditions. The atmospheric composition, temperature profile, and cirrus properties are the same as those used for Figure 1.8.

Figure 1.9a shows the upwelling infrared spectra at the top of the atmosphere under cloud-free and cirrus conditions. The atmospheric profiles and cirrus optical properties are the same as those used for Figure 1.8. For the infrared wavelengths the surface albedo was set to 0.01. The surface emissivity was, therefore, 0.99. The measure of wavelength used for Figure 1.9 is the wavenumber = 1/wavelength. The unit of wavenumber is "inverse centimeters" (cm^{-1}). A wavelength of 10 μm is the same as a wavenumber of 1000 cm^{-1}. A wavelength of 4 μm is the same as 2500 cm^{-1}. When speaking, one often uses 1000 "inverse centimeters" and 1000 "wavenumbers" interchangeably.

Water vapor absorbs at nearly all wavelengths associated with the Earth's infrared emission. The only exception is in the 8–12 μm infrared window, wavenumbers 850–1250 cm^{-1}. In the infrared window, water vapor absorbs only weakly. The major molecular absorption bands in the infrared are the rotation band of water vapor, 0–850 cm^{-1}; the 6.3 μm vibration–rotation band of water vapor, centered near 1590 cm^{-1}; the 15 μm vibration–rotation band of carbon dioxide, centered at 667 cm^{-1}; and the 9.6 μm vibration–rotation band of ozone,

centered near 1040 cm^{-1}. As was mentioned earlier, the properties of rotation and vibration–rotation bands are briefly described in Chapter 5.

The effect of the cirrus in the infrared is apparent in emission at the top of the atmosphere primarily in the infrared window. In the infrared window the cloud behaves similarly to a greenhouse gas. It absorbs radiation emitted by the surface and lower atmosphere and then emits radiation at a lower temperature. Just as in the window-gray model, because the cirrus is semitransparent at the window wavelengths, some of the radiation emitted by the surface and lower atmosphere is transmitted through the cirrus.

Figure 1.9b shows the infrared spectra emitted downward by the atmosphere at the surface. The downward emission is larger with the cirrus present than it is for cloud-free conditions. The increase in downward emission from cloudy skies during a cold, middle to high latitude winter night warms the surface by emitting radiation downward toward the surface. Under similar meteorological and cloud-free conditions, the surface rapidly cools by emitting radiation through the infrared window region. The cooling that results is so rapid that within a matter of minutes to an hour or so a temperature inversion builds up in the lowest portion of the atmosphere adjacent to the surface. The surface air becomes cold while the air above the inversion, sometimes only tens to a hundred meters from the surface, remains relatively warm.

Figure 1.10 presents another rendition of the surface and atmosphere energy budgets depicted by Trenberth and his coworkers [14]. These budgets are more accurate than those shown in Figure 1.7. In this depiction, the Earth is not in radiative equilibrium but absorbs sunlight at a rate that is slightly greater than the rate at which it emits infrared radiation. The additional sunlight heats the oceans at a rate of approximately 0.9 W m^{-2}. The radiative imbalance is due to the buildup of greenhouse gases in the atmosphere. The Earth is responding to this imbalance. Its temperature is rising, and it will continue to rise as long as the rate at which the Earth absorbs sunlight is greater than the rate at which it emits.

In addition to showing the various terms of the energy budget, Figure 1.10 also indicates the effect of clouds on the amount of sunlight reflected and radiation emitted. In the case of the radiation emitted, the 30 W m^{-2} emanating from clouds represents the net effect of the clouds on the Earth's emitted radiation. For scenes with no clouds, the global average radiation emitted at the top of the atmosphere is near 269 W m^{-2}, 30 W m^{-2} larger than the global average emission. This 30 W m^{-2} difference between the cloud-free and average emission is called the *cloud longwave radiative forcing*.

Table 1.3 provides estimates of the greenhouse forcing due to greenhouse gases, the infrared active gases in the Earth's atmosphere. The wavelengths at which these gases absorb overlap to varying degrees. The values in the table include the effects of the overlapping absorption by the gases. The estimates were calculated using a column model of the Earth's global average atmosphere [15] with a composition close to that described in Section 1.7. Surface emission was based on a global average surface temperature 288 K, giving an emission of 390 W m^{-2}. The top of the atmosphere emission was based on 2 years of observations from

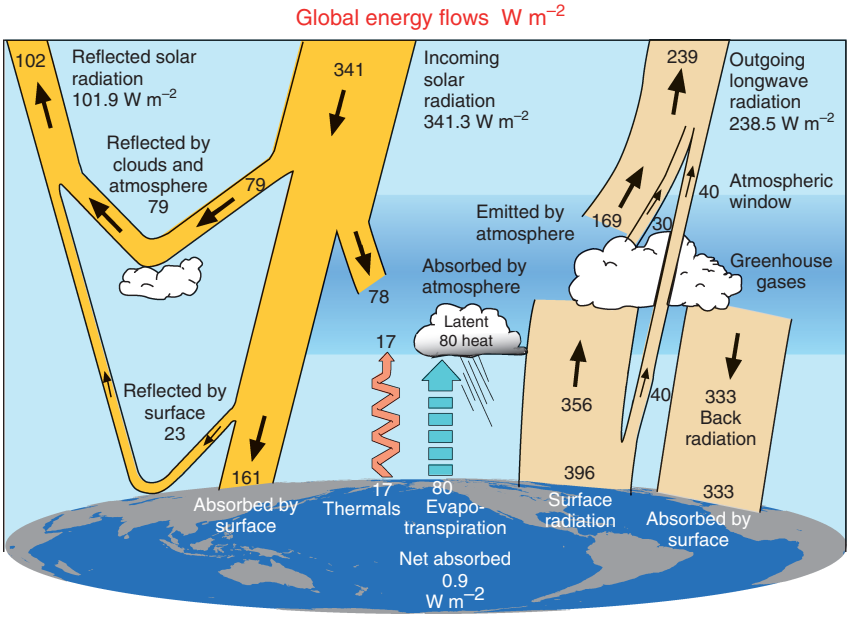

Figure 1.10 Earth's radiation budget based on 4 years of Earth radiation budget measurements by the NASA CERES project combined with model estimates based on global climate model radiation schemes and observations of the surface radiation budget, precipitation, runoff, and analyzed meteorological fields. (From Trenberth *et al.* [14], reproduced by permission of the American Meteorological Society.)

the NASA Earth's Radiation Budget Experiment (ERBE), 265 W m^{-2} for cloud-free scenes and 235 W m^{-2} for average cloudy conditions. The breakdown in the table shows that the greenhouse forcing of the gases is diminished considerably by the presence of clouds. With clouds present, the gases contribute only 86 W m^{-2}. The greenhouse forcing is $390 - 235$ W m^{-2} $= 155$ W m^{-2}. Consequently, clouds contribute $155 - 86$ W m^{-2} $= 69$ W m^{-2} to the forcing, making their contribution larger than any of the greenhouse gases.

In Figure 1.10, the 40 W m^{-2} that emanates from the surface represents the radiation emitted by the surface that is transmitted by the atmosphere. In Figure 1.7, this term is given as 10% of the incident sunlight. Most of this radiation passes through the infrared window at wavelengths between 8 and 12 μm. When present, clouds absorb most of this radiation emitted by the surface. They then emit radiation as a gray body with an emissivity near unity, so approximately similarly to a blackbody, at a temperature near that of the cloud tops. Most of the 30 W m^{-2} of the longwave cloud radiative forcing stems from the absorption and emission of radiation at wavelengths in the window region.

In the case of reflected sunlight, the term associated with the atmosphere and clouds includes scattering by molecules, which is Rayleigh scattering, and scattering by haze. Most of the scattering is due to molecules. Rayleigh scattering

Table 1.3 Estimates of the contribution by greenhouse gases and clouds to the greenhouse forcing by the Earth's atmosphere [15].

Gas	Cloud free ($W\,m^{-2}$)	Cloudy ($W\,m^{-2}$)
H_2O	75	51
CO_2	32	24
O_3	10	7
CH_4 and N_2O	8	4
Total	125	86

In these calculations the surface emission is $390\,W\,m^{-2}$, the top of the atmosphere emission is $235\,W\,m^{-2}$, and the greenhouse forcing is $155\,W\,m^{-2}$.

accounts for approximately 7% of the reflected sunlight, or about $24\,W\,m^{-2}$. Haze accounts for about 1–2% of the reflected sunlight, about $3–7\,W\,m^{-2}$. Clouds contribute the rest, or about $50–55\,W\,m^{-2}$. Adding the $\sim 29\,W\,m^{-2}$ of sunlight reflected by molecules and haze to the $23\,W\,m^{-2}$ contributed by the Earth's surface leads to reflected sunlight of $52\,W\,m^{-2}$, which is observed for cloud-free scenes by the NASA Cloud and Earth's Radiant Energy System (CERES) project [2]. As is the case for the greenhouse forcing, clouds dominate the Earth's reflected sunlight.

On the basis of the CERES observations, the annual average global cloudy sky reflected solar radiative flux is $99.5\,W\,m^{-2}$ [2]. The absorbed solar radiative flux for a cloudy Earth, $340.2 - 99.5\,W\,m^{-2} = 238.7\,W\,m^{-2}$; and that for a cloud-free Earth is $340.2 - 52\,W\,m^{-2} = 287.8\,W\,m^{-2}$. The change in the absorbed radiative flux in going from a cloudy Earth to a cloud-free Earth is $238.7 - 287.8\,W\,m^{-2} = -49.1\,W\,m^{-2}$, the cloud shortwave radiative forcing. The change in the absorbed sunlight due to the presence of clouds more than offsets the change in the emitted radiative flux. The net cloud radiative forcing is $-19.1\,W\,m^{-2}$. Clouds cool the Earth. With a climate sensitivity of $0.6\,K\,W^{-1}\,m^{-2}$, the Earth's annual mean global surface temperature would be more than 10 K higher without the clouds. The large values of the shortwave and longwave cloud radiative forcing make cloud feedbacks responsible for most of the current uncertainty in the Earth's climate sensitivity [4].

While the values in Figure 1.10 were based on "best estimates" of the various terms in the energy budget at the time the data were analyzed, many of the separate terms are rather uncertain. The $0.9\,W\,m^{-2}$ imbalance is thought to be within 15–20% of the actual imbalance. Release of latent heat in the atmosphere and evapotranspiration at the surface are based on observations of precipitation and may be uncertain by as much as 10–20%. The heating by dry turbulent exchange is based on analyzed meteorological data and is within 10%. The downward and reflected solar radiative fluxes and emission by the surface are known to be within 5%. The downward longwave emission from the atmosphere has an uncertainty of about 10%.

On the basis of known observational errors and estimates of uncertainties, 5 years of CERES observations were used to obtain optimal estimates of the top of the atmosphere radiative fluxes for cloud-free and average cloudy conditions [2]. The resulting estimates were constrained so that the net radiative imbalance equaled the rate at which the oceans were storing energy. The optimal estimates yielded values that differed to some extent from those shown in Figure 1.10. First, the incident sunlight, based on recent observations and a growing understanding of the errors in previous observations [1], is 340.2 W m^{-2}. The reflected sunlight is slightly less than portrayed in Figure 1.10, 99.5 W m^{-2}, and emission by the Earth is correspondingly larger, 239.6 W m^{-2}. Most of the uncertainties in these quantities stem from the calibration of the CERES instrument, ±2% for the reflected sunlight and ±1% for the emitted longwave radiation.

1.9 The Spatial Distribution of Radiative Heating and Circulation

Figure 1.11a shows the net shortwave radiative flux and Figure 1.11b shows the net longwave radiative flux at the top of the atmosphere. The fluxes have units of W m^{-2} and are 30 year averages (1971–2000) from a simulation with the National Center for Atmospheric Research (NCAR) Community Climate System Model 3 (CCSM3). The simulation is the "Climate of the 20th Century Experiment" (20C3M). The simulated data were obtained from the World Climate Research Program's (WCRP) Climate Model Intercomparison Project 3 (CMIP3) multi-model database [16]. The results in Figure 1.11 show considerable spatial variation in the net shortwave and longwave radiative fluxes, but these variations lie on top of much stronger latitudinal trends from equator to pole in both hemispheres.

Consider the consequences of the annual average incident solar radiation being a strong function of latitude. On the basis of solutions for radiative–convective equilibrium, regions at high latitudes with relatively large solar zenith angles are expected to be cold. Regions at low latitudes with relatively small solar zenith angles are expected to be warm. Because air expands as it is heated, at a given altitude the pressure for the cold regions at high latitudes will fall below those for the warm regions at low latitudes. A horizontal pressure gradient builds in the upper troposphere and the system becomes dynamically unstable. Circulation begins.

The circulation that arises strongly influences both the temperature and the moisture profile of the atmosphere. In addition to radiative and convective energy transfers, the zonal mean profiles now respond to dynamical contributions that arise from the atmospheric wind fields [17]. The changes to the temperature, moisture, and cloud fields that accompany the winds alter the radiative heating of the atmosphere and surface. Often, these changes work to enhance the circulation that first gave rise to the changes. For example, the Hadley circulation gets an extra

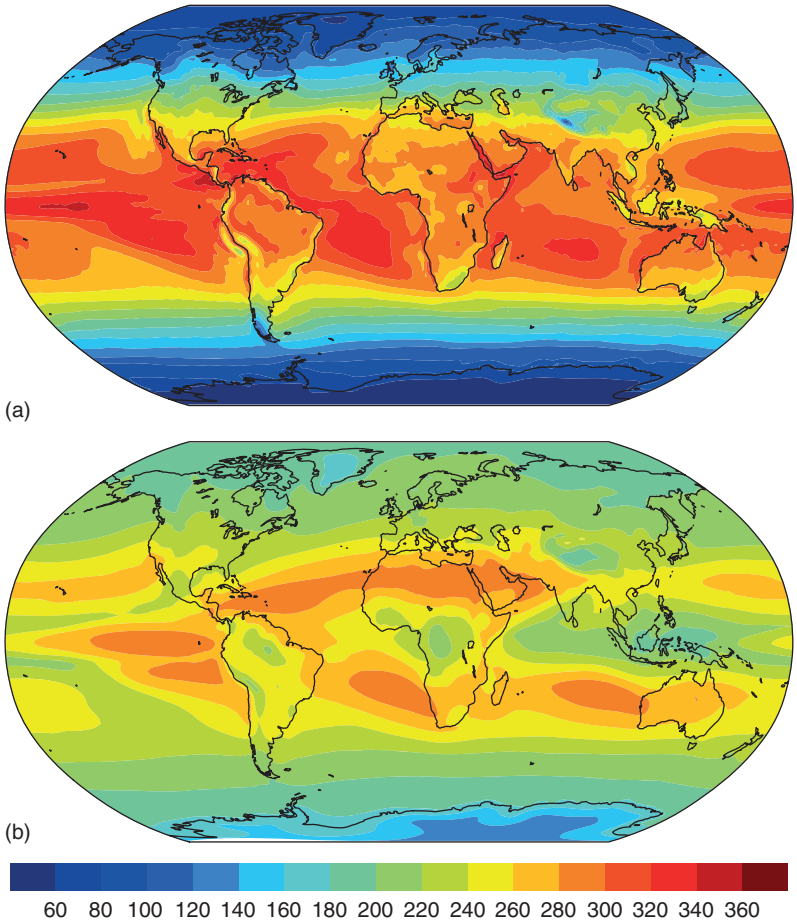

Figure 1.11 Net shortwave (a) and longwave (b) radiative fluxes in $W\,m^{-2}$ at the top of the atmosphere. They were obtained from a 30 year average (1971–2000) climate simulated with the NCAR CCSM3 as part of the "Climate of the 20th Century Experiment." The simulated data was obtained from the WCRP CMIP3 multi-model database [16].

boost from the release of latent heat at high altitudes in the tropics and the radiative cooling accompanying subsiding air in the subtropics. While complex numerical models appear to capture some of the feedbacks between circulation and radiation, such as in the Hadley circulation, they obviously miss subtler feedbacks, as for example, the maintenance of the large marine stratocumulus systems hanging over the eastern boundaries of the subtropical oceans in both northern and southern hemispheres.

As shown by the radiative fluxes in Figure 1.12, annually averaged, the solar radiation absorbed in the tropics is larger than the flux of infrared radiation emitted.

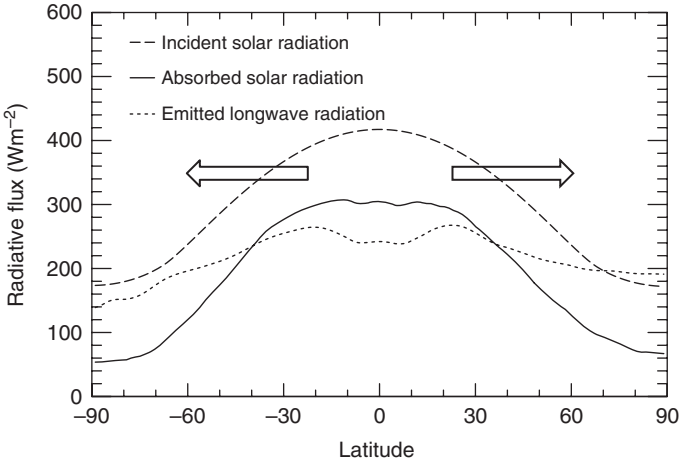

Figure 1.12 Annually averaged zonal mean incident shortwave, absorbed shortwave, and emitted longwave radiative fluxes from the 30 year averages for the NCAR CCSM3 20C3M experiment. The excess of absorbed sunlight over emitted infrared radiation in the tropics and the excess of emitted infrared radiation over absorbed sunlight at high latitudes reflect the poleward transport of energy from the tropics to the poles in both hemispheres as is indicated by the arrows. The dip in absorbed sunlight and emitted infrared radiation in the tropics marks the persistent location of the intertropical convergence zone and the associated deep convective clouds.

Similarly, the sunlight absorbed by the polar regions is smaller than the infrared radiation emitted by the regions. The circulation of the atmosphere and oceans transports energy from the tropics to higher latitudes, moderating the high temperatures in the tropics and the low temperatures in the polar regions.

Table 1.4 lists zonal mean radiative fluxes, albedos, and radiating temperatures for selected latitudes in the Northern Hemisphere. The observations are based on 11 years of the CERES Energy Balance and Filled (EBAF) data [2]. The "observed radiating temperatures" listed in the table are those of a blackbody that emits radiation at the rate given by the emitted zonally averaged infrared radiative flux. The radiative equilibrium temperature in the table is that given by a blackbody in radiative equilibrium with the zonally averaged absorbed solar radiation. In the tropics, the excess of the radiative equilibrium temperature over the observed radiating temperature indicates that the temperatures in the tropics are smaller than would be expected for radiative equilibrium. The smaller temperatures reflect the energy being lost to higher latitudes. At high latitudes, the excess of the observed radiating temperature over the radiative equilibrium temperature indicates that the temperatures in high latitudes are higher than would be expected for radiative equilibrium. The higher temperatures reflect the gain of energy being transported from lower latitudes.

Table 1.4 Annually and zonally averaged incident shortwave, absorbed shortwave, and emitted longwave radiative fluxes, radiative equilibrium temperatures, and observed radiating temperatures for selected Northern Hemisphere latitudes.

Latitude	Incident sunlight ($W\,m^{-2}$)	Albedo	Absorbed sunlight ($W\,m^{-2}$)	Emitted infrared ($W\,m^{-2}$)	Equilibrium radiating temperature (K)	Observed radiating temperature (K)
10°N	410	0.24	311	247	272	257
20°N	391	0.24	297	270	269	262
30°N	364	0.28	263	257	261	259
40°N	327	0.32	222	235	250	253
50°N	283	0.38	176	219	236	249
60°N	235	0.41	139	210	222	246
70°N	195	0.49	100	201	205	244

The values are averages from 11 years of CERES-EBAF data.

1.10 Summary and Outlook

This chapter focused on simple radiative equilibrium and window-gray models that behave similar to the Earth and its atmosphere. The remainder of the book explores more deeply the nature of radiation, the scattering and absorption of sunlight, the absorption and emission of infrared radiation, and how the radiative terms shown in Figures 1.7 and 1.10 are calculated. It also explores the ways in which the reflected and transmitted sunlight and emitted infrared radiation at selected wavelengths can be used to infer the composition of the atmosphere and its thermodynamic structure. The narrative begins with the nature of light (Chapter 2) and how it interacts with matter as it propagates through scattering, absorbing, and emitting media (Chapter 3). The propagation, tied to a frame of reference, such as the Earth's surface, leads to the equation of radiative transfer. Simple solutions are then developed for the transfer of infrared radiation and sunlight, including the effects of multiple scattering (Chapter 4). The solutions set the stage for making simple estimates of the radiative terms in Figures 1.7 and 1.10. Obtaining accurate estimates of the terms, however, requires the integration of solutions to the radiative transfer equation over all wavelengths from the short UV wavelengths to the long thermal infrared wavelengths. The calculations are cumbersome and require many details involving molecular absorption spectra. Simplifications are made that capture the essence of the absorption by molecules so that calculations using the simplified solutions can be performed over finite bands of wavelengths (Chapter 5). These simplifications are then applied to calculate the contributions to the Earth's albedo by haze, clouds, ozone, and water vapor (Chapter 6). They are then applied to calculate the change in emission caused by a doubling of carbon dioxide in the Earth's atmosphere and how this doubling not

only leads to a warming of the Earth and its atmosphere, but also a cooling of the stratosphere (Chapter 7).

Problems

1. Based on the values given in Figure 1.7, calculate the following:

a. Use the apparent transmissivity of the troposphere to calculate an effective emissivity for longwave radiation.
b. Use the emissivity calculated in (a) to calculate an apparent radiating temperature for the downward emission at the surface.
c. Use the effective radiating temperature obtained in (b) to calculate the apparent altitude of the emitting layer. Use the emission at the surface to obtain the surface temperature and assume a tropospheric lapse rate of $\Gamma = 6.5\,\mathrm{K\,km^{-1}}$ to obtain the apparent altitude.
d. Repeat the calculations in (b) and (c), but for the upward radiation emitted by the troposphere at the tropopause.
e. Explain why the emissivity and temperatures obtained in (a – d) differ from those obtained with the window-gray, radiative equilibrium model.
f. Repeat (a – d) for the stratosphere. Consider the stratosphere to start at an altitude of 15 km and the temperature of the lower stratosphere to be 205 K. Assume a stratospheric lapse rate of $\Gamma = -2\,\mathrm{K\,km^{-1}}$. A negative lapse rate indicates that temperature rises with altitude in the stratosphere.
g. Assume a tropopause pressure of 250 hPa and calculate the net *radiative* cooling (K/day) for the troposphere.
h. The net radiative cooling of the troposphere is approximately compensated by the release of latent heat when water condenses and falls as precipitation. Calculate the rate of precipitation (mm/day) required to just balance the net radiative cooling. Use $2.5 \times 10^6\,\mathrm{J\,kg^{-1}}$ for the heat of vaporization for water. Compare this approximate estimate of the precipitation rate with the rate of surface evaporation.
i. Assume that the stratosphere represents all of the atmosphere above 250 hPa and calculate the heating rate of the stratosphere (K/day) caused by the absorption of sunlight by O_3.
j. Assume a global average surface albedo of 0.1 and calculate the incident sunlight ($\mathrm{W\,m^{-2}}$) at the surface. What surface albedo would contribute the $23\,\mathrm{W\,m^{-2}}$ to the Earth's reflected sunlight shown in Figure 1.10? Estimate the albedo to two significant figures.

2. By integrating the cosine of the solar zenith angle over the surface of the sunlit side of the Earth, show that the global average cosine for the solar zenith angle of the sunlit Earth is 0.5. Consequently, a suitable value of the "average solar zenith angle" for the sunlit side of the Earth is 60°.

3. Construct a window-gray, radiative equilibrium model for the Earth's atmosphere in which 20% of the incident sunlight is absorbed by the atmosphere.

Assume that the albedo for the Earth is 0.3 and the surface temperature is 288 K. Assume that the atmosphere *absorbs* the incident sunlight but *reflects* none of it.

a. Calculate the surface albedo that is consistent with an Earth albedo of 0.3 and a nonreflecting atmosphere that absorbs 20% of the incident sunlight. Account for the absorption of sunlight as it passes through the atmosphere to the surface and the absorption of the sunlight that is reflected by the surface that passes through the atmosphere to space.
b. Is the emissivity obtained for an atmosphere that absorbs sunlight greater or smaller than the emissivity for an atmosphere that absorbs none of the incident sunlight?
c. Is the atmospheric temperature of the absorbing atmosphere greater than the temperature for an atmosphere that absorbs none of the incident sunlight?

4. Estimate the amplitude of the day–night temperature difference for a window-gray, radiative equilibrium model of Mars. The Earth and Mars have nearly identical rotation rates. Use the following steps:

a. Calculate the emissivity of the Martian atmosphere on the basis of the appropriately reduced solar constant, the albedo, and the surface temperature.
b. Calculate the radiative time constant as the e-folding time for cooling after the sun has been removed.
c. Calculate the temperature perturbation for $t = 12$ h.
d. What does your estimate of the day–night difference for Mars suggest about the likely relationship between diurnally forced temperature changes and weather-related temperature changes on Mars?

	Earth	Mars
Relative distance to the sun	1.0	1.52
Albedo	0.30	0.15
Surface temperature (K)	288	240
Surface pressure (hPa)	1013.25	7
Heat capacity, C_p ($\mathrm{J\,kg^{-1}\,K^{-1}}$)	1005	830
Acceleration due to gravity, g ($\mathrm{m\,s^{-2}}$)	9.80	3.76

5. Develop a time-dependent version of the global average radiative equilibrium model as given by Equation 1.5 to determine the response of the Earth's radiating temperature following the 1991 Mt. Pinatubo eruption. The eruption caused a perturbation in the albedo that initially amounted to a $4\,\mathrm{W\,m^{-2}}$ decrease in the sunlight absorbed by the Earth. Assume that the albedo is

given by

$$\alpha = \alpha_0 + \alpha' \exp\left(-\frac{t}{\tau_a}\right)$$

with $\alpha_0 = 0.30$ the global average albedo and α' the change in the albedo required to produce the $4\,\mathrm{W\,m^{-2}}$ decrease in absorbed sunlight at $t = 0$. Assume $\tau_a = 2$ years for the residence time of the haze layer that formed in the stratosphere after the eruption. Use the following steps to obtain a time-dependent solution for the Earth's radiating temperature.

a. Expand the Stefan–Boltzmann law in the radiative equilibrium model about its initial equilibrium state. As was done for the window-gray model in Section 1.6, use a first-order perturbation method to obtain the change in the Earth's radiating temperature as a function of time following the Mt. Pinatubo eruption. Assume that the change in the radiating temperature approximates the changes in the lower atmospheric and surface temperatures. Use the heat capacity of air and the mass per unit area of the atmosphere to represent the thermal inertia of the system. Solve for the temperature change as a function of time after the eruption and use it to determine when the minimum occurred and the decrease in the surface temperature at the minimum.
b. Repeat these calculations using the thermal inertia of the ocean mixed layer. Use 50 m as the depth of the mixed layer and $4218\,\mathrm{J\,kg^{-1}\,K^{-1}}$ as the heat capacity of water. The temperature change for the ocean mixed layer produces a more realistic response.
c. Repeat (a) and (b) but instead of the Earth's radiating temperature and the Stefan-Boltzmann law, assume that the emitted longwave flux is given by $F = A + BT_S$ with A and B constants and T_S the annually averaged global mean surface temperature. Assume that $B = 2\,\mathrm{W\,m^{-2}K^{-1}}$. As with the radiating temperature, assume that the change in the average surface temperature approximates the change in the temperature of the lower troposphere. How does including a feedback comparable to that of the water vapor feedback alter the minimum surface temperature and the delay between the eruption and the minimum?
   The Earth's surface temperature decreased to approximately 0.4 K and this minimum was reached approximately 1.3 years after the Mt. Pinatubo eruption.

6. Derive equations for a two-layered, window-gray, radiative equilibrium model. Give the layers arbitrary emissivities $\varepsilon_1 > 0$ and $\varepsilon_2 > 0$ with $\varepsilon_1 \neq \varepsilon_2$. Show algebraically that for radiative equilibrium, the temperature of the upper atmospheric layer must be less than that of the lower layer and the temperature of the surface must be greater than that of the lower atmospheric layer. Consequently, within the simple window-gray radiative equilibrium model, temperature must fall with increasing altitude.

References

1. Kopp, G., Lawrence, G., and Rottman, G. (2005) The total irradiance monitor (TIM): Science results. *Solar Phys.*, **230**, 129–140.
2. Loeb, N.G., Wielicki, B.A., Doelling, D.R., Smith, G.L., Keyes, D.F., Kato, S., Manalo-Smith, N., and Wong, T. (2009) Toward optimal closure of the Earth's top-of-atmosphere radiation budget. *J. Clim.*, **22**, 748–766.
3. Pippard, A.B. (1957) *Elements of Classical Thermodynamics for Advanced Students of Physics*, Cambridge University Press, Cambridge.
4. Solomon, S., Qin, D., Manning, M., Alley, R.B., Bernstein, T., Bindoff, N.L., Chen, Z., Chidthaisong, A., Gregory, J.M., Nicholls, N., Heimann, J.M., Hewitson, B., Hoskins, B.J., Joos, F., Jouzei, J., Kattsov, V., Lohmnn, U., Matsuno, T., Molina, M., Nicholls, N., Overpeck, J., Raga, G., Ramaswamy, V., Ren, J., Rusicucci, M., Sommerville, R., Stocker, T.F., Whetton, P., Wood, R.A., and Wratt, D. (2007) Technical summary, in *Climate Change, 2007: The Physical Science Basis. Contribution of Working Group I to the Fourth Assessment Report of the Intergovernmental Panel on Climate Change* (eds S. Solomon, D. Qin, M. Manning, Z. Chen, M. Marquis, K.B. Averyt, M. Tignor, and H.L. Miller), Cambridge University Press, Cambridge, New York.
5. Soden, B.J. and Held, I.M. (2006) An assessment of climate feedbacks in coupled ocean-atmosphere models. *J. Clim.*, **19**, 3354–3360.
6. Manabe, S. and Strickler, R.F. (1964) Thermal equilibrium of the atmosphere with convective adjustment. *J. Atmos. Sci.*, **21**, 361–385.
7. Manabe, S. and Wetherald, R.T. (1967) Thermal equilibrium of the atmosphere with a given distribution of relative humidity. *J. Atmos. Sci.*, **24**, 241–259.
8. Green, A.E.S. (1964) Attenuation by ozone and the Earth's albedo in the middle ultraviolet. *Appl. Opt.*, **3**, 203–208.
9. Lacis, A.A. and Hansen, J.E. (1974) A parameterization for the absorption of solar radiation in the earth's atmosphere. *J. Atmos. Sci.*, **31**, 118–133.
10. Goody, R.M. and Yung, Y.L. (1989) *Atmospheric Radiation*, Oxford University Press, Oxford.
11. Houghton, J.T. (2002) *The Physics of Atmospheres*, Cambridge University Press, Cambridge.
12. Hartmann, D.L. (1994) *Global Physical Climatology*, Academic Press, San Diego, CA.
13. Baum, B.A., Yang, P., Heymsfield, A.J., Platnick, S., King, M.D., Hu, Y.X., and Bedka, S.M. (2005) Bulk scattering properties for the remote sensing of ice clouds. II: narrowband models. *J. Appl. Meteorol.*, **44**, 1896–1911.
14. Trenberth, K.E., Fasullo, J.T., and Kiehl, J.T. (2009) Earth's global energy budget. *Bull. Am. Meteorol. Soc.*, **90**, 311–323.
15. Kiehl, J.T. and Trenberth, K.E. (1997) Earth's annual global mean energy budget. *Bull. Am. Meteorol. Soc.*, **78**, 197–208.
16. Information concerning the 20C3M experiment can be found at, *http://www-pcmdi.llnl.gov/projects/cmip/ann_20c3m.php*.
17. Trenberth, K.E. and Smith, L. (2009) The three dimensional structure of the atmospheric energy budget: methodology and evaluation. *Clim. Dyn.*, **32**, 1065–1079.